Hindawi Publishing Corporation
Journal of Computational Engineering
Volume 2016, Article ID 6762390, 24 pages
http://dx.doi.org/10.1155/2016/6762390

Research Article

Best L_1 Piecewise Monotonic Data Approximation in Overhead and Underground Medium-Voltage and Low-Voltage Broadband over Power Lines Networks: Theoretical and Practical Transfer Function Determination

Athanasios G. Lazaropoulos

School of Electrical and Computer Engineering, National Technical University of Athens, 9 Iroon Polytechniou Street, 15780 Zografou, Greece

Correspondence should be addressed to Athanasios G. Lazaropoulos; aglazaropoulos@gmail.com

Received 19 March 2016; Revised 17 July 2016; Accepted 19 July 2016

Academic Editor: Marek Krawczuk

This paper investigates the efficiency and accuracy of the best L_1 piecewise monotonic data approximation (best L1PMA) in order either to approximate the transfer functions of distribution BPL networks or to reveal the aforementioned transfer functions when various faults occur during their determination. The contribution of this paper is quadruple. First, based on the inherent piecewise monotonicity of distribution BPL transfer functions, a piecewise monotonic data approximation is first applied in BPL networks; best L1PMA is outlined and applied during the determination of distribution BPL transfer functions. Second, suitable performance metrics such as the percent error sum (PES) and fault PES are reported and applied so as to assess the efficiency and accuracy of the best L1PMA during the determination of distribution BPL transfer functions. Third, the factors of distribution BPL networks that influence the performance of best L1PMA are identified. Fourth, the accuracy of the best L1PMA is assessed with respect to its inherent properties, namely, the assumed number of monotonic sections and the nature of faults, that is, faults that follow either continuous uniform distribution (CUD) or normal distribution (ND), during the determination of distribution BPL transfer functions. Finally, best L1PMA may operate as the necessary intermediate antifault method for the theoretical and practical transfer function determination of distribution BPL networks.

1. Introduction

Electrical power industry at the beginning of the 21st century is facing a variety of technological and economic challenges. The rising cost of energy, the mass electrification of everyday life, the integration of distributed energy sources, microgrids, demand side management, and climate change are the major drivers that will determine the speed at which the modernization of power distribution grid—that is, either overhead or underground, either MV or LV power grids—will occur [1, 2]. Taking into consideration the inevitability of this oncoming massive change, SG technologies are fervently embraced by the electrical power industry [3].

Towards that direction, the deployment of BPL networks across the entire distribution grid can help towards the evolution of the vintage power system to an advanced IP-based power network supported by a plethora of SG applications [4–6]. Actually, distribution BPL networks may provide the required broadband communications framework for different SG services and applications such as better power grid management, home and wide-area networking, advanced metering infrastructure, and more accurate demand response programs [7–12]. However, distribution BPL networks considerably differ in their topological and circuital characteristics from other wireline communication networks [13, 14]. Distribution BPL networks suffer from attenuation, multipath, and noise, each significantly affecting their network design [4, 15–17].

Apparently, the introduction of appropriate channel models to determine transfer functions of distribution BPL

networks at high frequencies remains a challenging issue since the distribution power grid was not originally designed to deliver broadband services and applications. The well-known hybrid method, which is usually adopted to describe the spectral behavior of different BPL networks, is also employed in this paper [4, 13–21]. On the basis of its accurate results, a variety of factors affecting transfer functions of distribution BPL networks are identified, namely, the type of distribution power grid, that is, either overhead or underground, either MV or LV, the topology of the distribution BPL network, the MTL configuration, and the applied coupling scheme, that is, how the BPL signal is injected into power lines. However, despite the fact that a plethora of experimental results and theoretical analyses validate the theoretical accuracy of the hybrid method [22–26], a number of practical reasons and "real-life" conditions may create significant differences between experimental measurements and theoretical results during the transfer function determination of distribution BPL networks. On the basis of six fault categories, which are analytically reported in the following analysis, their impact on the transfer functions of distribution BPL networks is evaluated and analyzed.

In order either to approximate the transfer functions of distribution BPL networks or to mitigate the aforementioned faults that occurred, the best L1PMA is first applied in BPL networks. Among the myriad of data approximation methods that has been proposed in the literature, the application of the proposed best L1PMA, which is theoretically presented and experimentally verified in [27–32], is adopted in this paper due to its remarkable efficiency to cope with problems that are derived from univariate signal restoration. In fact, best L1PMA avoids the assumption that transfer functions depend on certain critical parameters and only focuses on the smallest change to the transfer function data such that the first differences of the approximated transfer function data are allowed to change their sign only a prescribed number of times [28, 29]. In accordance with [33], best L1PMA receives as inputs the measured transfer function and the number of monotonic sections that are presented across the transfer function in the examined frequency band while it gives as output the approximated transfer function. Exploiting the inherent piecewise monotonicity of distribution BPL transfer functions, best L1PMA can comfortably accommodate the undulation of the transfer function data due to the attenuation, multipath, noise, and other faults. In addition, a fact worth mentioning is that the Fortran software package, which had been developed in order to implement the best L1PMA, has extensively been verified in various scientific fields [30, 33] and is freely available online in [33].

In order to evaluate the approximation accuracy of best L1PMA during the theoretical determination of transfer functions, the performance metric of PES is proposed in this paper. PES calculates the total sum of the relative differences between the approximated transfer function of best L1PMA and the theoretical transfer function in the examined frequency range. Compared against the fault PES, which computes the total sum of the relative differences between the measured transfer function and the theoretical transfer function in the examined frequency range, the impact of several factors on the accuracy of best L1PMA, such as the distribution power grid type, the distribution BPL network topology, the applied coupling scheme, the number of monotonic sections, and the distribution followed by the faults that occurred, is recognized and assessed.

The rest of the paper is structured as follows. In Section 2, a brief presentation of the overhead and underground MV/BPL and LV/BPL networks is shown. Special attention is given to the used MTL configurations and distribution BPL topologies as well as the fundamental knowledge regarding BPL signal propagation and transmission across distribution BPL networks. In Section 3, a presentation of the best L1PMA is given. Implementation details, mathematical analysis, and PES concerning best L1PMA are analytically reported. Section 4 discusses simulations of various distribution BPL networks intending to mark out the efficiency of best L1PMA either to approximate the transfer functions of distribution BPL networks or to mitigate the faults that occurred due to measurements and noise. Section 5 concludes this paper.

2. Presentation of Overhead and Underground MV/BPL and LV/BPL Networks: MTL Configurations, BPL Topologies, and Propagation/Transmission Analysis

2.1. The Overhead MV and LV Power Grids. The overhead MV and LV distribution lines, which are examined in this paper, are shown in Figures 1(a) and 1(b), respectively. Overhead MV distribution line consists of three parallel noninsulated phase conductors, which are spaced by Δ_{MV} and hang at h_{MV} above ground, whereas overhead LV distribution lines comprise four parallel noninsulated conductors, which are spaced by Δ_{LV} and located at h_{LV} above ground for the lowest conductor. As regards the overhead MV distribution line configuration, it consists of ACSR three-phase conductors [4, 13, 14]. In the case of the overhead LV distribution line, it consists of ASTER three-phase conductors while the upper conductor is the neutral conductor [4]. Exact values concerning conductor properties and configuration geometries are reported in [1].

The ground is considered as the reference conductor with conductivity σ_g and relative permittivity ε_g that are assumed equal to 5 mS/m and 13, respectively. The former ground properties define a realistic scenario [4, 13–15, 34, 35]. The impact of imperfect ground on broadband signal propagation across power lines was studied in [13, 34–36].

2.2. The Underground MV and LV Power Grids. The underground MV and LV lines, which are examined in this paper, are presented in Figures 1(c) and 1(d), respectively. The underground MV and LV lines are the three-phase sector-type PILC distribution-class cable and the three-phase four-conductor core-type YJV/XLPE underground LV distribution cable, respectively. Both underground MV and LV distribution lines are considered to be buried 1 m inside the ground with the same ground properties as described in Section 2.1. More analytically, when the underground MV distribution line is concerned, its cable arrangement

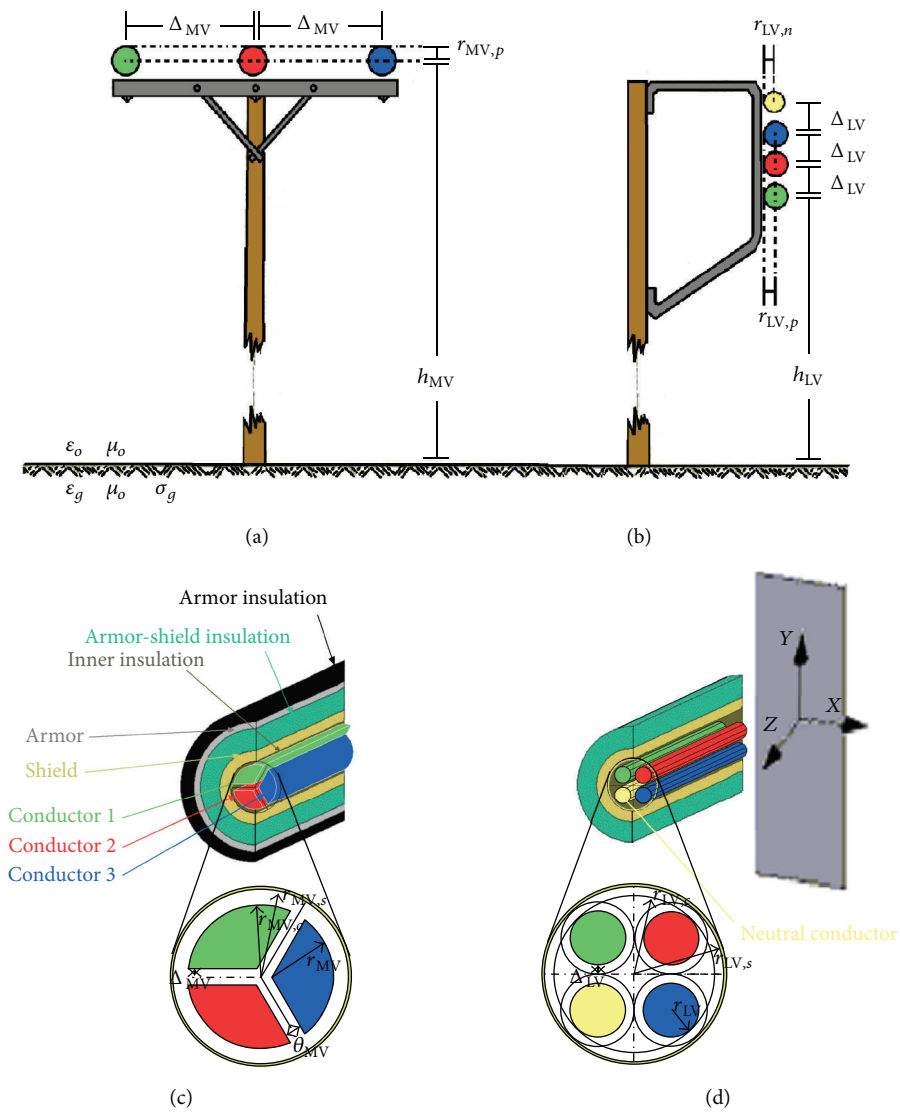

Figure 1: Typical MTL structures [1, 4]. (a) Overhead MV. (b) Overhead LV. (c) Underground MV. (d) Underground LV.

consists of the three-phase three-sector-type conductors, one shield conductor, and one armor conductor. In the case of underground LV distribution line, the cable arrangement comprises the three-phase three-core-type conductors, one core-type neutral conductor, and one shield conductor. In both underground distribution lines, the shield and the armor are grounded at both ends [4, 15, 37]. Thus, the shield acts as a ground return path and is considered as the reference conductor [4, 19, 38]. Exact values concerning conductor properties and configuration geometries are reported in [1, 4, 19, 38–41]. Broadband transmission via underground distribution power lines has been detailed in [15, 19, 39, 40, 42] where the analytical formulation considered in this paper has been analyzed.

Here, it should be noted that the type of the underground MV cable, which is examined in this paper, cannot be characterized as the typical case. In fact, most modern underground MV cables are usually single-core laid in horizontal or trefoil arrangements. However, the PILC cable is one of the oldest types of power cables being used for almost one hundred years. Shielded PILC cables are still dominant for urban applications in many countries (e.g., most larger North American urban centers, Netherlands, and Malaysia) and are extensively used for power distribution, not only at the MV but also at the LV level [15, 37, 38]. Therefore, the paper focuses on the propagation via PILC cables—rather than via XLPE cables which present lower attenuation—because PILC cables behave closer to the LOS transmission behavior of the majority of existing underground MV grids. Thus, an indicative picture of the real-world situation will be obtained [37, 38].

2.3. Topologies of Distribution BPL Networks. In accordance with [1, 4, 17], average path lengths of 1000 m and 200 m are typically encountered in overhead and underground distribution BPL topologies, respectively. During the following

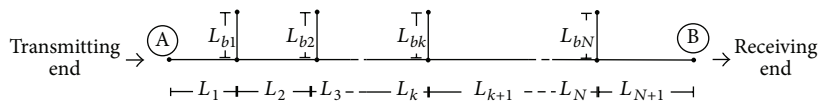

Figure 2: End-to-end distribution BPL topology with N branches.

analysis, the distribution BPL network of Figure 2 having N branches is considered.

With reference to Figure 2, five indicative overhead distribution BPL topologies of average path length, which are reported in Table I of [1], are examined, namely, (i) overhead urban case A, (ii) overhead urban case B, (iii) overhead suburban case, (iv) overhead rural case, and (v) overhead "LOS" case. Note that this topology corresponds to the Line-of-Sight transmission—that is, no branches are encountered across the BPL signal transmission path. In accordance with [1, 4, 17], these five indicative topologies are assumed to be common across overhead distribution BPL networks regardless of their type.

Similar to overhead distribution BPL case, five indicative underground distribution BPL topologies of average path length, which are reported in Table II of [1], are examined in this paper, namely, (i) urban case A, (ii) urban case B, (iii) underground suburban case, (iv) underground rural case, and (v) underground "LOS" case. Similar to overhead distribution BPL networks, these five indicative topologies are assumed to be common across underground distribution BPL networks regardless of their type [4, 16, 17].

With reference to Figure 2, the distribution and branching TLs are assumed to be identical while their interconnections are considered to be fully activated. In addition, the transmitting and the receiving ends are assumed to be matched to the characteristic impedance of distribution TLs, whereas the branch terminations are assumed to be open circuits [4, 13, 14, 16–18, 43–45].

2.4. The Basics of the BPL Signal Propagation in Overhead and Underground Distribution BPL Networks. Analytically described in [1, 4, 13–21, 39, 40, 46–49], the standard TL analysis, which involves two conductors, can be extended to the MTL analysis, which involves more than two conductors, through a straightforward matrix approach. Actually, compared to the two-conductor line of standard TL analysis, which supports one forward- and one backward-traveling wave, a MTL structure with $n + 1$ conductors supports n pairs of forward- and backward-traveling waves. Each pair of forward- and backward-traveling waves is referred to as a mode and is characterized by its propagation constant. As the distribution MTL configurations of Figures 1(a)–1(d) are concerned, overhead and underground MV MTL structures may support three ($n = 3$) modes, whereas overhead and underground LV MTL structures may support four ($n = 4$) modes.

In order to describe the propagation of modes across distribution BPL networks, the hybrid method, which is analytically demonstrated in [4, 13, 14, 16–18, 46], describes the spectral relationship between $V_i^m(z)$, $i = 1, \ldots, n$, and $V_j^m(0)$, $j = 1, \ldots, n$, introducing the operators $H_{i,j}^m\{\cdot\}$, $i, j = 1, \ldots, n$, so that

$$\mathbf{V}^m(z) = \mathbf{H}^m\{\mathbf{V}^m(0)\}, \tag{1}$$

where $\mathbf{V}^m(z) = [V_1^m(z) \cdots V_n^m(z)]^T$ are the voltages of the n modes supported by the considered distribution MTL configuration (modal voltages), $[\cdot]^T$ denotes the transpose of a matrix, $\mathbf{H}^m\{\cdot\}$ is the $n \times n$ modal transfer function matrix whose elements $H_{i,j}^m\{\cdot\}$, $i, j = 1, \ldots, n$, are the modal transfer functions, and $H_{i,j}^m$ denotes the element of matrix $\mathbf{H}^m$ in row i of column j.

2.5. The Basics of the BPL Signal Transmission in Distribution BPL Networks. In accordance with [1, 14, 20, 21, 34, 35], the BPL signal can be injected into overhead and underground distribution lines through the following two coupling scheme types, namely, (i) *WtG and StP coupling schemes* (in the case of WtG coupling schemes, the signal is injected into one conductor of the examined overhead MTL configuration and returns via the ground; the WtG coupling scheme between conductor s and the ground will be denoted by WtG^s; in the case of StP coupling schemes, the signal is injected into one conductor of the examined underground MTL configuration and returns via the shield; the StP coupling scheme between conductor s and the shield will be denoted by StP^s) and (ii) *WtW or PtP coupling schemes* (the signal is injected between two conductors of the examined MTL configuration; in the case of overhead MTL configurations, WtW coupling schemes between conductors p and q will be denoted by $\mathrm{WtW}^{p\text{-}q}$, whereas, in the case of underground MTL configurations, PtP coupling schemes between conductors p and q will be denoted by $\mathrm{PtP}^{p\text{-}q}$).

Based on (1), the theoretical coupling transfer function $H^X\{\cdot\}$ is given by

$$H^X\{\cdot\} = \left[\mathbf{C}^X\right]^T \cdot \mathbf{T}_V \cdot \mathbf{H}^m\{\cdot\} \cdot \mathbf{T}_V^{-1} \cdot \mathbf{C}^X, \tag{2}$$

where $[\cdot]^X$ denotes the applied coupling scheme, $\mathbf{C}^X$ is the $n \times 1$ coupling column vector analyzed in [4], and $\mathbf{T}_V$ is an $n \times n$ matrix depending on the frequency, the geometry of the examined MTL configuration, and the physical properties of the cables used [1, 4, 6, 14, 21, 38, 42, 46, 50–56].

2.6. Differences between Theory and Practice during the Determination of Transfer Functions of Distribution BPL Networks. Although a plethora of experimental results and derived theoretical analyses validate the theoretical accuracy of the aforementioned modeling approach [22–26], a set of practical reasons and "real-life" conditions may create significant differences between experimental measurements and

theoretical results during the transfer function determination of distribution BPL networks. More specifically, these fault factors can be classified into the following six fault categories, namely [48, 52, 57], (i) difficulties of isolating specific MTL parameters from time- and frequency-domain reflectometry measurements, (ii) the sensitivity and accuracy of the used measurement equipment, (iii) resonant effects and cross talk phenomena due to parasitic capacitances and inductances, (iv) the weakness of including specific wiring and grounding practices, (v) practical impedance deviations of branch terminations and transmitting/receiving ends, and (vi) the lack of absolutely isolating the effect of noise during the transfer function computations. Taking into consideration these fault categories and (2), the measured coupling transfer function $\overline{H^X}\{\cdot\}$ is determined by

$$\overline{H^X}(f) = H^X(f) + e(f), \tag{3}$$

where f denotes the measurement frequency and $e(f)$ synopsizes the total fault that occurred due to the aforementioned six fault categories.

To mitigate the faults that occurred, which can seriously impair the accuracy of transfer function modeling, the best L1PMA is adopted so that the theoretical transfer functions can be restored.

3. Best L1PMA

3.1. Brief Presentation of Best L1PMA. During the last 70 years, the monotonic problem has attracted significant interest from many academic fields, such as engineering, health, economics, and statistics, as well as from various applications, including signal restoration, spectroscopy, image processing, and art [29, 58–65]. Among the various proposed monotonic data approximation methods, the application of the best L1PMA, which is theoretically presented and experimentally verified in [27–32], successfully copes with problems that are derived from univariate signal restoration. This is due to the fact that this approximation method focuses on the smallest change to the data such that the first differences of the smoothed data change sign a prescribed number of times.

When the application of best L1PMA is concerned with the intention of restoring theoretical coupling transfer functions of distribution BPL networks behind the total faults that occurred due to the six fault categories of Section 2.6, some advantages that are gained by implementing this approximation method are given; namely, (i) observing the behavior of transfer functions of distribution BPL networks [1, 4, 13–17, 66–71], piecewise monotonicity is a property that always occurs due to the intrinsic BPL propagation and transmission drawbacks, such as "LOS" attenuation and multipath environment; exploiting this inherent BPL network property, best L1PMA is decomposed into optimal monotonic computations in the sections between adjacent turning points (local extrema) of transfer functions [29, 32]; (ii) contrary to spline and wavelet approximation methods presented in [72, 73], best L1PMA avoids the assumption that transfer functions depend on certain critical parameters; actually, the smoothing process is a straightforward data projection when best L1PMA is adopted [28, 29]; (iii) already demonstrated in [28, 29, 32], best L1PMA is particularly suitable for mitigating large and uncorrelated data errors; since best L1PMA is based on the minimization of the moduli sum of the data errors, the existence of few gross errors among the data makes no difference to the best fit [74]; therefore, the undulation of the coupling transfer function data due to the existence of deep spectral notches and other faults can be comfortably accommodated through the application of the best L1PMA; and (iv) the Fortran software package that is applied in order to implement the best L1PMA has extensively been verified in various scientific fields [30, 32, 63–65] and is freely available online in [33].

3.2. Mathematical Implementation of Best L1PMA in Distribution BPL Transfer Functions. With reference to (3), the measured coupling transfer functions $\overline{H^X}(f_i)$, $i = 1, \ldots, u$, with respect to measurement frequencies f_i, $i = 1, \ldots, u$, are regarded as elements of $\overline{\mathbf{H}^X}$, where

$$\overline{\mathbf{H}^X} \equiv \overline{\mathbf{H}^X}(\mathbf{f}) = \left[\overline{H^X}(f_1) \cdots \overline{H^X}(f_u)\right]^T \tag{4}$$

is the $u \times 1$ measured coupling transfer function column vector and $\mathbf{f} = [f_1 \cdots f_u]^T$ is the $u \times 1$ measurement frequency column vector.

Based on the specifications of Fortran software package of [33], best L1PMA receives as inputs the measured coupling transfer function column vector $\overline{\mathbf{H}^X}$, the measured frequency column vector $\mathbf{f}$, the number of monotonic sections k_{sect} that is provided either by the user or automatically by the computer, and the type of the first monotonic section (i.e., either increasing or decreasing). Note that, in the case of the coupling transfer functions of distribution BPL networks, the first monotonic section is always decreasing. Then, by executing the Fortran software package, which is a straightforward procedure, best L1PMA automatically derives the optimal local extrema as well as the best fit. Actually, best L1PMA gives as output the $u \times 1$ approximated coupling transfer function column vector $\overline{\overline{\mathbf{H}^X}} \equiv \overline{\overline{\mathbf{H}^X}}(\mathbf{f}) = [\overline{\overline{H^X}}(f_1) \cdots \overline{\overline{H^X}}(f_u)]^T$ whose elements $\overline{\overline{H^X}}(f_i)$, $i = 1, \ldots, u$, are the approximated coupling transfer functions for the given measurement frequencies f_i, $i = 1, \ldots, u$, respectively. In fact, best L1PMA calculates the approximated coupling transfer function column vector $\overline{\overline{\mathbf{H}^X}}$ by minimizing the sum of the moduli of the errors that are given by

$$\operatorname{Er}\left(\overline{\mathbf{H}^X}\right) = \sum_{i=1}^{u} \left|\overline{\overline{H^X}}(f_i) - \overline{H^X}(f_i)\right| \tag{5}$$

subject to the piecewise monotonicity constraints

$$\begin{aligned} &\overline{\overline{H^X}}\left(f_{\phi_{j-1}}\right) \le \overline{\overline{H^X}}\left(f_{\phi_{j-1}+1}\right) \le \cdots \le \overline{\overline{H^X}}\left(f_{\phi_j}\right), \\ &\qquad\qquad \text{if } j \text{ is odd}, \\ &\overline{\overline{H^X}}\left(f_{\phi_{j-1}}\right) \ge \overline{\overline{H^X}}\left(f_{\phi_{j-1}+1}\right) \ge \cdots \ge \overline{\overline{H^X}}\left(f_{\phi_j}\right), \\ &\qquad\qquad \text{if } j \text{ is even}, \end{aligned} \tag{6}$$

where the integer numbers ϕ_j, $j = 1, \ldots, k_{\text{sect}}$, define the positions of the local extrema of the best L1PMA satisfying the conditions

$$1 = \phi_0 \leq \phi_1 \leq \cdots \leq \phi_{k_{\text{sect}}} = u. \tag{7}$$

3.3. Mathematical Assessment of Best L1PMA in Distribution BPL Transfer Functions. As it has already been mentioned in Section 3.2, the number of monotonic sections k_{sect}, which is an input to the best L1PMA, can be provided either manually by the user or automatically by the computer. To evaluate the approximation accuracy of best L1PMA to the theoretical coupling transfer function for the different values of monotonic sections, a new performance metric is proposed in this paper. More specifically, the PES expresses as a percentage the total sum of the relative differences between the approximated coupling transfer function and the theoretical coupling transfer function for all the used frequencies; namely,

$$\text{PES} \equiv \text{PES}\left(k_{\text{sect}}\right) = \frac{\sum_{i=1}^{u} \left|\overline{\overline{H^X}}\left(f_i\right) - H^X\left(f_i\right)\right|}{\sum_{i=1}^{u} \left|H^X\left(f_i\right)\right|}. \tag{8}$$

On the basis of (8), PES helps towards (i) the evaluation of the approximation accuracy of the best L1PMA to the theoretical coupling transfer function when different numbers of monotonic sections are considered and (ii) the evaluation of the restoration degree of the theoretical coupling transfer function offered by best L1PMA when faults occur due to the six fault categories.

With respect to (3), to assess the best L1PMA mitigation efficiency towards the faults, PES of (8) is compared against the fault PES that is given by

$$\text{PES}_{\text{fault}} = \frac{\sum_{i=1}^{u} \left|\overline{H^X}\left(f_i\right) - H^X\left(f_i\right)\right|}{\sum_{i=1}^{u} \left|H^X\left(f_i\right)\right|}. \tag{9}$$

4. Numerical Results and Discussion

Various types of distribution BPL networks are simulated with the purpose of investigating the efficacy of the best L1PMA during the transfer function restoration when various faults occur. More specifically, the efficiency of the best L1PMA is assessed based on the changes incurred by a number of factors, such as the type of distribution power grid, the distribution BPL topology, the applied coupling scheme, and the nature of faults (i.e., fault distributions).

As regards the simulation specifications, the BPL frequency range and flat-fading subchannel frequency spacing are assumed to be equal to 1–30 MHz and 1 MHz, respectively. Therefore, the number of subchannels u in the examined frequency range is equal to 30. This implies that the theoretical maximum number of monotonic sections that can occur during the application of the best L1PMA is equal to 29 [29, 30].

To simplify the analysis without, however, harming its generality, in the case of overhead and underground MV/BPL networks, only WtG^1/StP^1 and $\text{WtW}^{1\text{-}2}$/$\text{PtP}^{1\text{-}2}$ coupling schemes will be examined, hereafter. As it is usually done [1, 4, 17, 19, 20, 46], the selection of representative coupling schemes is a typical procedure for the sake of reducing manuscript size.

4.1. Distribution BPL Topologies and Best L1PMA. Prior to understanding the significant fault restoration delivered by adopting best L1PMA, there is a need for recognizing best L1PMA accuracy in approximating theoretical coupling transfer functions of distribution BPL topologies.

In Figures 3(a)–3(e), the theoretical coupling transfer function is plotted versus frequency for the five indicative overhead MV/BPL topologies, respectively, when WtG^1 coupling scheme is applied. In each figure, the best L1PMA is also plotted for a number of representative monotonic sections (i.e., $k_{\text{sect}} = 2$, $k_{\text{sect}} = 5$, and $k_{\text{sect}} = 20$). In Figures 3(f)–3(j), similar curves to Figures 3(a)–3(e) are shown when $\text{WtW}^{1\text{-}2}$ coupling scheme is adopted. In Figures 4(a)–4(j), similar plots to Figures 3(a)–3(j) are given but for overhead LV/BPL networks.

In Figures 5(a)–5(e), the theoretical coupling transfer function is plotted versus frequency for the five indicative underground MV/BPL topologies, respectively, when StP^1 coupling scheme is adopted. In each figure, the best L1PMA is also plotted for the same number of representative monotonic sections as in Figures 3(a)–3(e). In Figures 5(f)–5(j), similar plots to Figures 5(a)–5(e) are curved when $\text{PtP}^{1\text{-}2}$ coupling scheme is applied. In Figures 6(a)–6(j), similar plots to Figures 5(a)–5(j) are given in the case of underground LV/BPL networks.

Observing Figures 3(a)–3(j), 4(a)–4(j), 5(a)–5(j), and 6(a)–6(j), several interesting remarks can be pointed out:

(i) Already mentioned in [1, 4, 9, 13–17, 19, 71, 75], the spectral behavior of the transfer functions depends drastically on the frequency, the type of the examined distribution power grid, the applied coupling scheme, the physical properties of the MTL configuration, and the path length as well as the number and the length of the branches.

(ii) The presence of branches along the end-to-end transmission path causes signal reflections and a multipath environment that further creates spectral notches in the coupling transfer functions. The number, the extent, and the depth of the spectral notches that occurred depend on the number and the length of the branches. It should be noted that the spectral notches are superimposed on the "LOS" attenuation.

(iii) Based on the behavior of spectral notches in the coupling transfer functions, distribution BPL topologies can be categorized into three channel classes as follows [1, 4, 15, 16, 71]:

(a) *Bad Channel Class.* BPL transmission in many urban zones (i.e., urban cases A and B) belongs to this channel class. This channel class is characterized by topologies with a high number of branches of small electrical length. Due

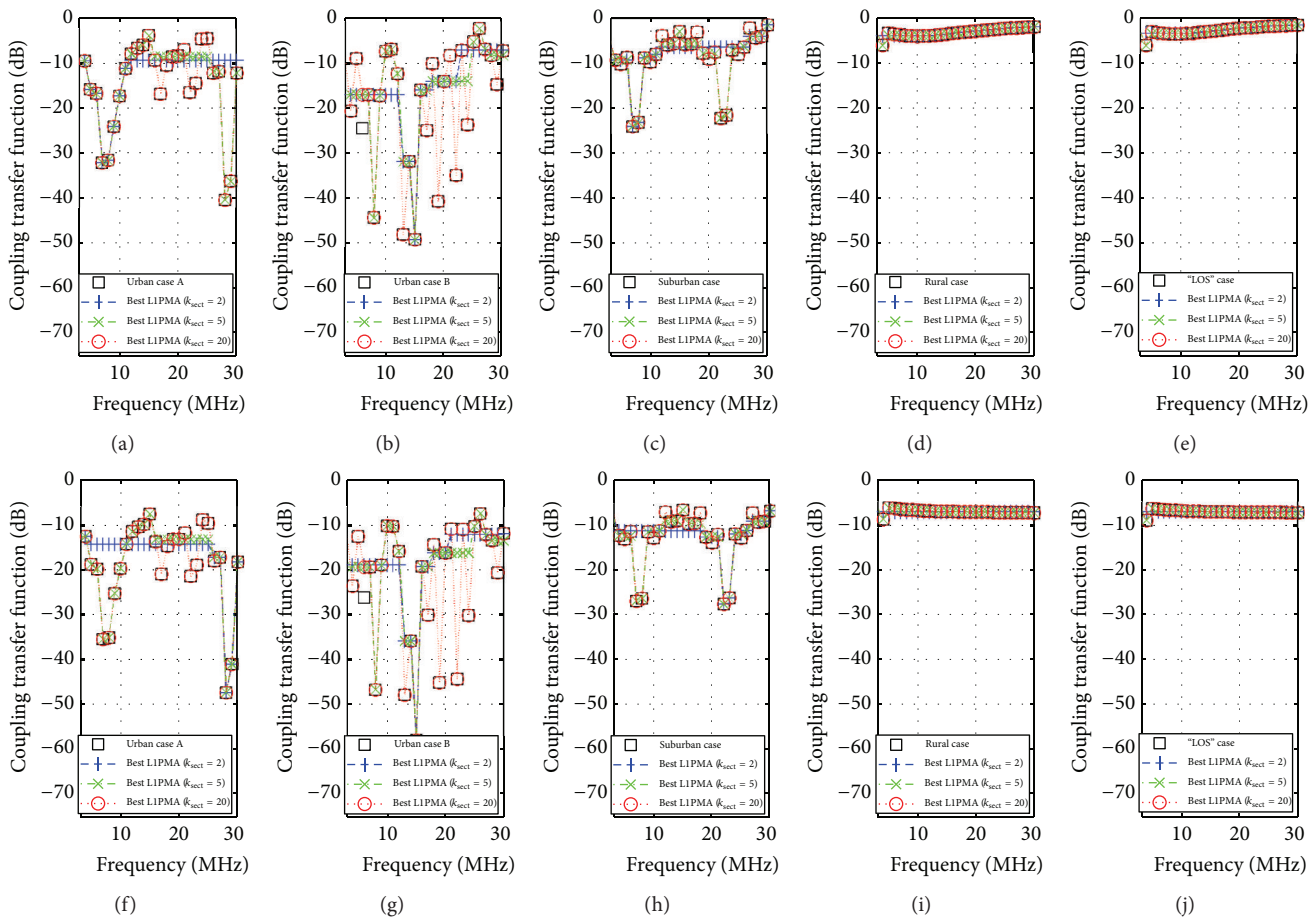

Figure 3: Coupling transfer function of the five indicative topologies of overhead MV/BPL networks when different coupling schemes are applied and various best L1PMAs are adopted. (a)–(e) WtG^1 coupling scheme. (f)–(j) $WtW^{1\text{-}2}$ coupling scheme.

to the aggravated multipath environment that occurred, deep and frequent spectral notches are noticed in coupling transfer functions.

(b) *Good Channel Class*. BPL transmission in suburban and rural areas belongs to this channel class. Shallow spectral notches are observed in coupling transfer functions due to the relatively low number of long branches.

(c) *"LOS" Channel Class*. This class represents the end-to-end transmission when no intermediate branches exist. Apart from the "LOS" attenuation, no spectral notches are observed.

(iv) Regardless of the applied coupling scheme and the examined distribution power grid type, best L1PMA remarkably approximates the examined coupling transfer functions of all the channel cases as follows:

(a) Best L1PMA curves practically coincide with the coupling transfer functions of "LOS" channel class. The absence of spectral notches and the monotonous form of "LOS" attenuation allowed the best L1PMA to perfectly fit the coupling transfer functions of this channel class by simply using only few monotonic sections (i.e., lower than 5).

(b) Best L1PMA accurately describes the behavior of the coupling transfer functions of good channel class as well as their spectral notches. Actually, the shallow spectral notches of coupling transfer functions are treated by the best L1PMA as monotonous sections of decreases and increases. Hence, best L1PMA succeeds in including in its best fit the vast majority of the local extrema. Therefore, the number of monotonic sections, which is required by the best L1PMA to accurately describe the coupling transfer functions of good channel class, is higher than the respective one of "LOS" channel class.

(c) Best L1PMA satisfactorily describes the spectral behavior of bad channel class. Although the coupling transfer functions of this channel class are characterized by deep and frequent spectral notches, best L1PMA succeeds in including the majority of these local extrema in its fits. In

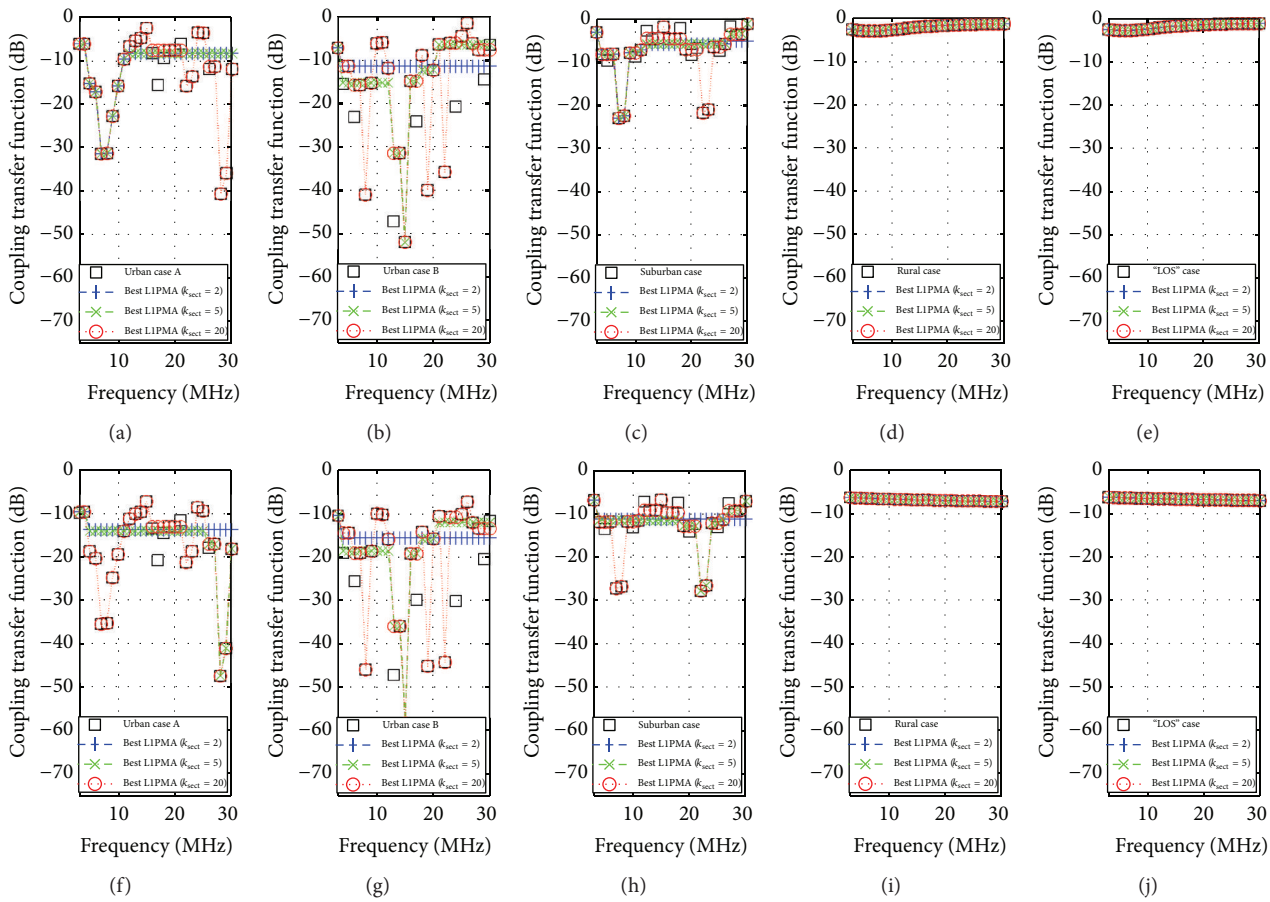

FIGURE 4: Same as in Figures 3(a)–3(j) but for overhead LV/BPL networks.

order to adequately describe these intense spectral fluctuations, it is obvious that best L1PMA exploits all the available monotonic sections; for example, best L1PMA uses more than 20 monotonic sections—see Figures 3(a)–3(j), 4(a)–4(j), 5(a)–5(j), and 6(a)–6(j).

(v) Best L1PMA successfully achieves representing either the local extrema or the tail of coupling transfer functions. In contrast with wavelet or spline approximations [72, 73], best L1PMA manages to mitigate perturbations (ripples) into the tail of the approximation when a great number of extrema occur [28, 59, 60, 76].

From the previous analysis, it is evident that the number of monotonic sections determines the approximation efficiency of best L1PMA to the coupling transfer functions of distribution BPL networks. In order to highlight this critical role, PES is plotted versus the number of monotonic sections in Figure 7(a) for the five indicative topologies of overhead MV/BPL networks when WtG^1 and $WtW^{1\text{-}2}$ coupling schemes are considered. In Figures 7(b)–7(d), same plots are given in the case of overhead LV/BPL, underground MV/BPL, and underground LV/BPL networks, respectively. Note that, in the case of underground distribution BPL networks, StP^1 or $PtP^{1\text{-}2}$ coupling schemes are applied instead of WtG^1 or $WtW^{1\text{-}2}$ ones, respectively.

From Figures 7(a)–7(d), it is evident that the perfect fit of best L1PMA primarily depends on the number of monotonic sections. Actually, there are an optimal number of monotonic sections above which the improvement of PES remains marginal. This optimal number depends on (i) the distribution power grid type; (ii) the number, the extent, and the depth of spectral notches of the coupling transfer function (i.e., the channel class of the examined distribution BPL topology); and (iii) the applied coupling scheme. As already mentioned, although this optimal number of monotonic sections is low when distribution BPL topologies of "LOS" and good channel class are examined, it presents significant higher values when distribution BPL topologies of bad channel class are investigated. Taking into account the upper limit of the number of monotonic sections, even if best L1PMA does not perform its best fit to the data in order to coincide with the coupling transfer functions of bad channel class, it satisfactorily approximates them. Through the prism of PES and in order to assess the accuracy of best L1PMA, the optimal number of monotonic sections is presented in Table 1 for the cases examined in Figures 7(a)–7(d). Note that the optimal number of monotonic sections is defined for given best L1PMA execution scenario when PES of the examined scenario takes for the first time the value 10^{-3}% or less.

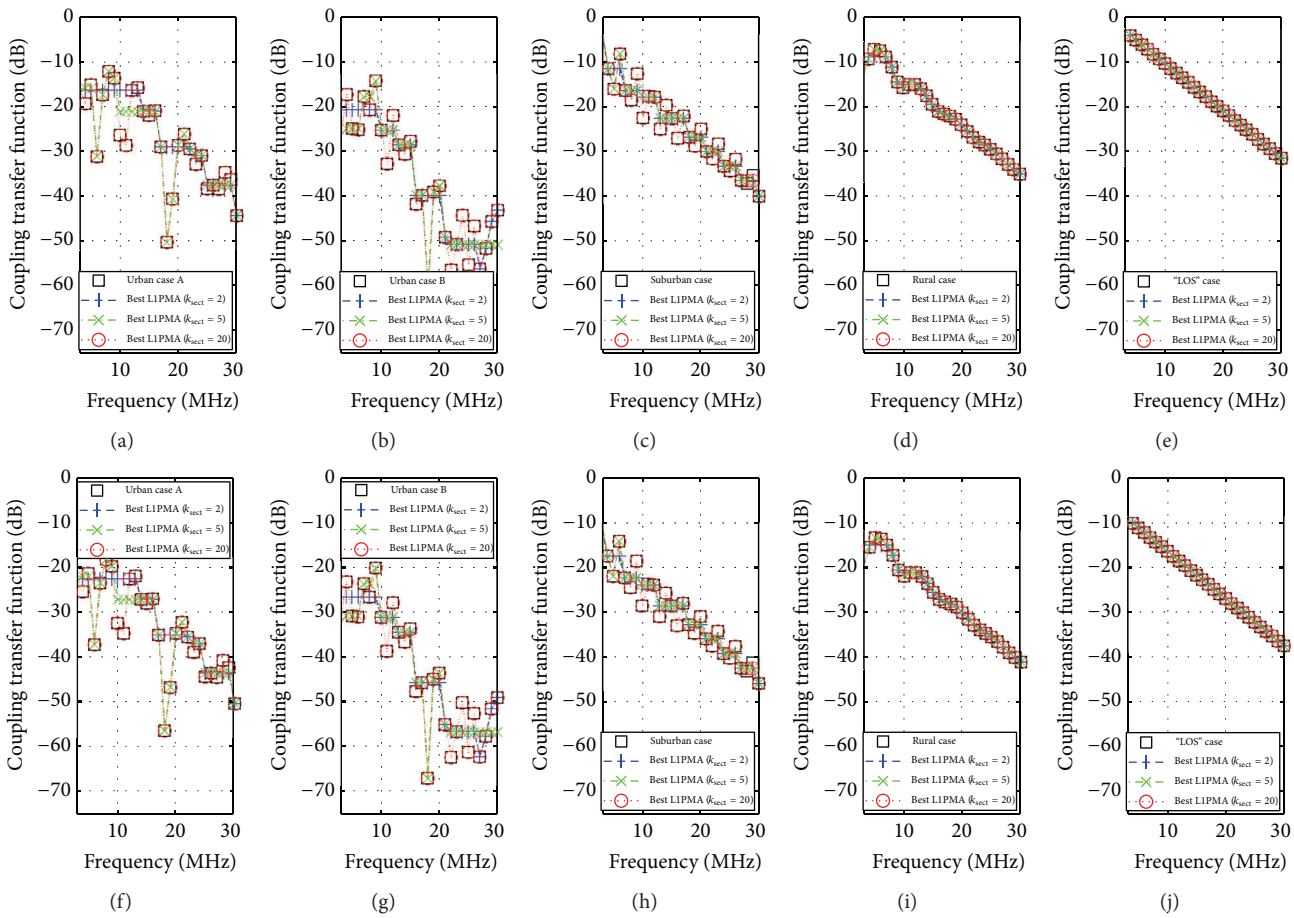

FIGURE 5: Coupling transfer function of the five indicative topologies of underground MV/BPL networks when different coupling schemes are applied and various best L1PMAs are adopted. (a)–(e) StP^1 coupling scheme. (f)–(j) $PtP^{1\text{-}2}$ coupling scheme.

From Table 1, it is numerically validated that the best L1PMA succeeds in accurately fitting coupling transfer functions of distribution BPL topologies in all the cases examined. PES results indicate that the best L1PMA can successfully approximate either the trend of "LOS" attenuation or the deep spectral notches that occurred due to the multipath environment. As it has already been outlined, the optimal number of monotonic sections increases when distribution BPL topologies of bad channel class are investigated and remains low when distribution BPL topologies of "LOS" and good channel class are examined.

As the optimal number of monotonic sections is concerned, the following remarks are pointed out:

(i) In 15% of the cases examined, best L1PMA has achieved fitting coupling transfer functions with optimal number of monotonic sections greater than 20.

(ii) In 25% of the cases examined, best L1PMA has fitted coupling transfer functions with optimal number of monotonic sections lower than 5.

(iii) In general terms, the average PES of best L1PMA is equal to $0.99 \times 10^{-5}\%$ which is an extremely low value in comparison with the applied PES threshold of $10^{-3}\%$. This fact implies that best L1PMA perfectly fits theoretical coupling transfer functions.

Since the optimal number of monotonic sections uniquely describes the pattern of the coupling transfer function of each distribution BPL topology, this number is going to characterize each distribution BPL topology towards its coupling transfer function restoration when faults occur as presented in the following section.

4.2. Best L1PMA against Faults during the Determination of Theoretical Coupling Transfer Function of Distribution BPL Networks. As it has already been reported in Section 2.6, there are six fault categories that can create significant differences between experimental measurements and theoretical results during the determination of coupling transfer function of distribution BPL networks. As it is shown in this section, based on the approximation efficiency of best L1PMA, the theoretical coupling transfer function of distribution BPL networks can be revealed even though significant faults may occur. On the basis of the optimal number of monotonic sections, which has been determined in Table 1 for each distribution BPL network topology and coupling scheme, best L1PMA achieves mitigating the additive faults

Table 1: Optimal number of monotonic sections and PES for distribution BPL networks (OV: overhead; UN: underground).

		Urban case A		Urban case B		Suburban case		Rural case		"LOS" case	
		Number of monotonic sections k_{sect}	PES($\times 10^{-5}$%)	Number of monotonic sections k_{sect}	PES($\times 10^{-5}$%)	Number of monotonic sections k_{sect}	PES($\times 10^{-5}$%)	Number of monotonic sections k_{sect}	PES($\times 10^{-5}$%)	Number of monotonic sections k_{sect}	PES($\times 10^{-5}$%)
OVMV	WtG^{1}	12	1.2	22	0.9	20	0.7	6	0.7	6	0.7
	$WtW^{1\text{-}2}$	14	1.3	22	1.0	20	1.5	5	0.3	5	0.5
OVLV	WtG^{1}	10	1.0	21	0.7	20	0.6	2	1.2	2	1.4
	$WtW^{1\text{-}2}$	14	1.5	21	1.1	20	1.4	1	0.4	1	0.4
UNMV	StP^{1}	19	0.9	20	0.7	22	1.0	5	1.1	1	1.1
	$PtP^{1\text{-}2}$	19	0.7	20	0.7	22	1.1	5	1.1	1	1.0
UNLV	StP^{1}	16	1.0	20	1.1	18	1.4	1	0.9	1	0.8
	$PtP^{1\text{-}2}$	16	1.3	20	1.1	18	1.2	1	1.4	1	1.5

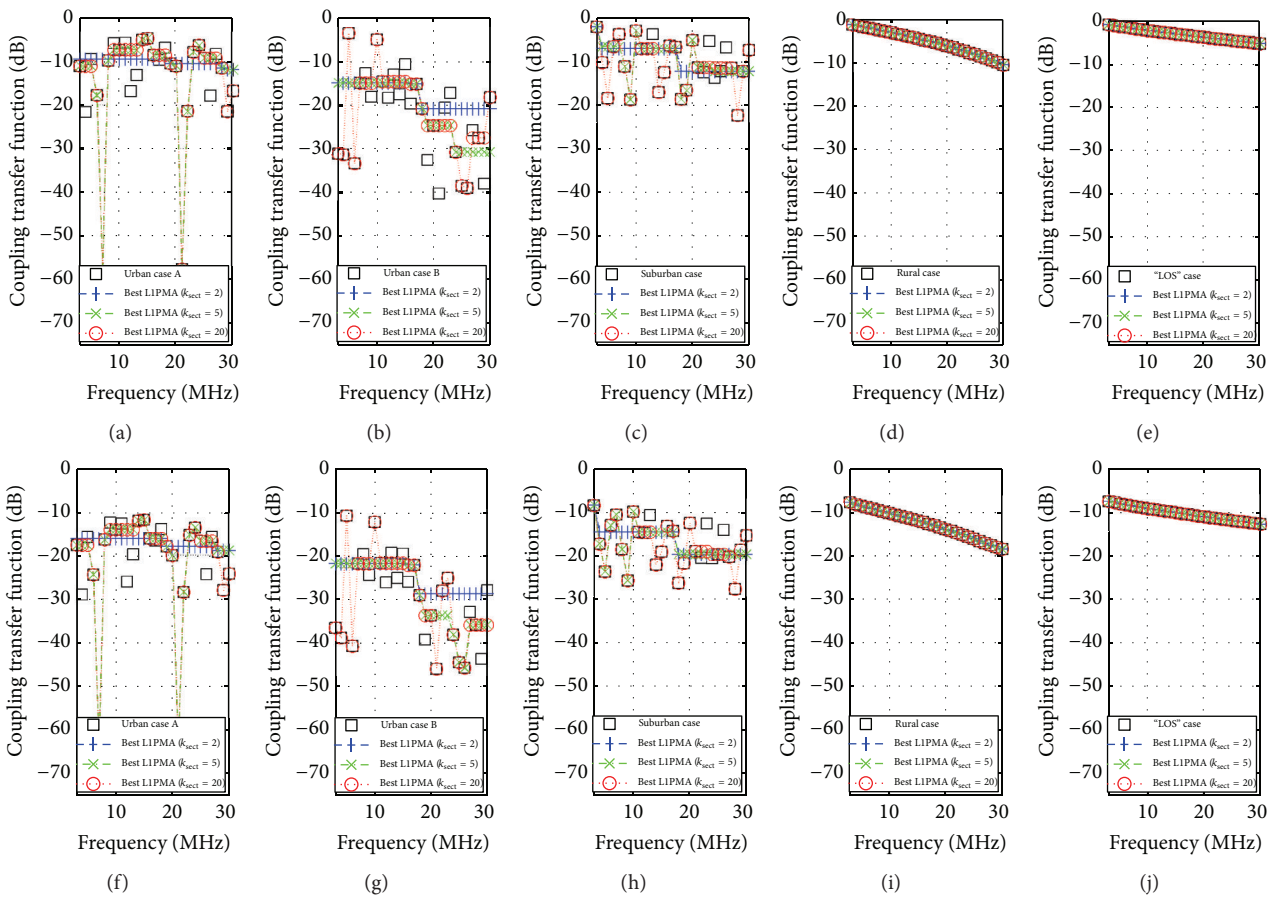

FIGURE 6: Same as in Figures 5(a)–5(j) but for underground LV/BPL networks.

by simply maintaining the monotonicity pattern of each coupling transfer function. In fact, the fault effect can be drastically counterbalanced since best L1PMA relies on the median of the corresponding data within a range. In the following analysis, the total fault that occurred due to the six fault categories $e\{\cdot\}$, which is described in (3), is assumed to follow either CUD with minimum value $-\alpha_{\mathrm{CUD}}$ and maximum value α_{CUD} or ND with mean μ_{ND} and standard deviation σ_{ND}.

To examine the impact of faults on the determination of coupling transfer function of distribution BPL networks, in Figures 8(a)–8(e), the theoretical coupling transfer function is plotted versus frequency for the five indicative overhead MV/BPL topologies, respectively, when WtG^1 coupling scheme is applied. In each figure, the measured coupling transfer function is also drawn with faults that are characterized by the following indicative distributions, namely, (i) CUD with $\alpha_{\mathrm{CUD}} = 6\,\mathrm{dB}$ and (ii) ND with $\mu_{\mathrm{ND}} = 0\,\mathrm{dB}$ and $\sigma_{\mathrm{ND}} = 2\,\mathrm{dB}$. Moreover, the best L1PMA is also curved for the two previous measured coupling transfer functions. In Figures 8(f)–8(j), similar curves to Figures 8(a)–8(e) are plotted when $\mathrm{WtW}^{1\text{-}2}$ coupling scheme is adopted. In Figures 9(a)–9(j), 10(a)–10(j), and 11(a)–11(j), similar plots to Figures 8(a)–8(j) are given in the case of overhead LV/BPL networks, underground MV/BPL networks, and underground LV/BPL networks, respectively. Note that, in the case of underground distribution BPL networks, StP^1 or $\mathrm{PtP}^{1\text{-}2}$ coupling schemes are applied instead of WtG^1 or $\mathrm{WtW}^{1\text{-}2}$ ones, respectively.

From Figures 3(a)–3(j), 4(a)–4(j), 5(a)–5(j), and 6(a)–6(j), it has been pointed out that best L1PMA identifies the most important local extrema of theoretical coupling transfer functions, while interpolating the data at these extrema. The increase of the number of monotonic sections allows best L1PMA to make the sum of the squares of the residuals smaller while maintaining the most important local extrema of the theoretical coupling transfer function. In Figures 8(a)–8(j), 9(a)–9(j), 10(a)–10(j), and 11(a)–11(j), best L1PMA relies on the number of monotonic sections provided by the theoretical coupling transfer functions [29]. Inversely, given the number of the monotonic sections, best L1PMA first tries to pinpoint the most important local extrema of measured coupling transfer functions and second performs the best fit among the data in every monotonous section. Actually, best L1PMA makes the sum of the squares of the residuals smaller, while maintaining the most important local extrema.

Moreover, in the attempt to provide structure in data assuming that there is no underlying mathematical function, the assumption of the specific number of monotonic sections seems to be quite important and accurate. In fact, this assumption can substitute the trend test algorithm of [77]

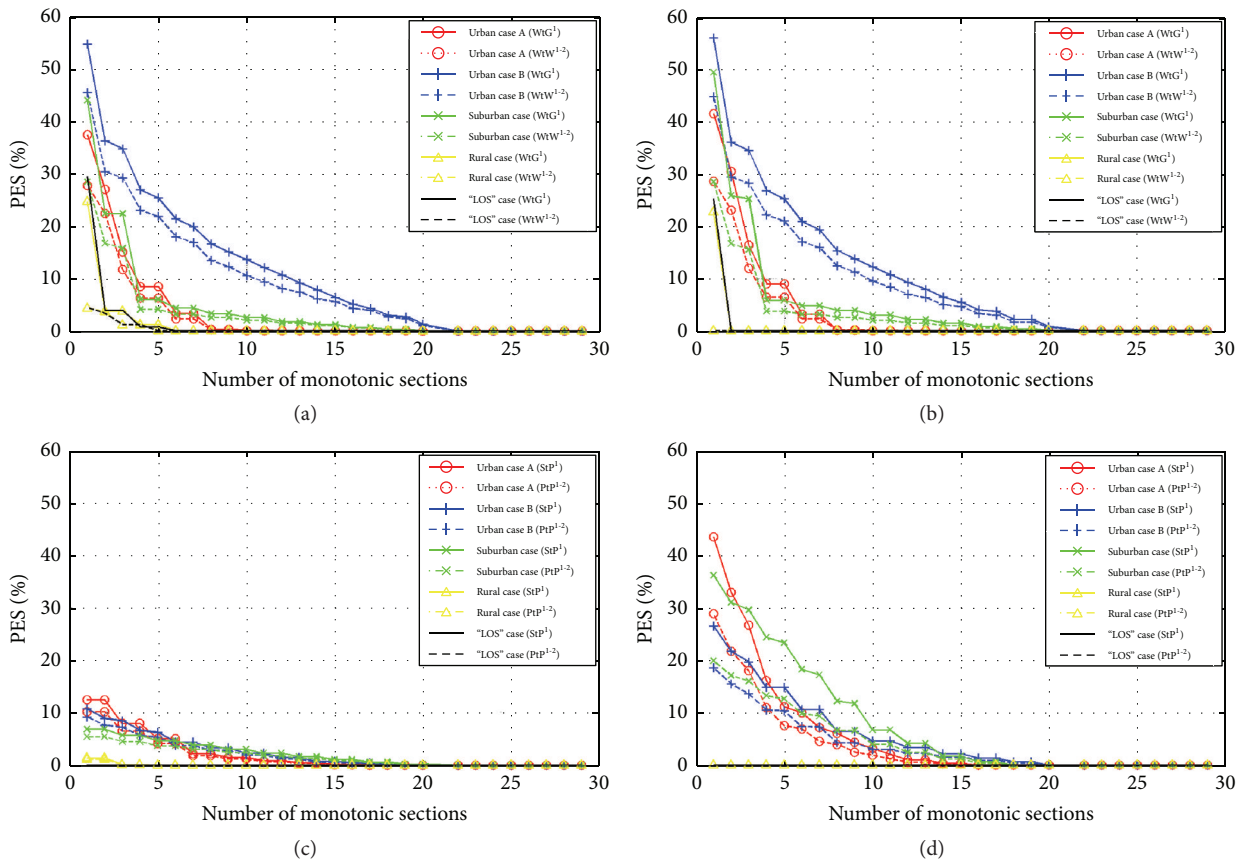

Figure 7: PES of distribution BPL topologies when various coupling schemes are applied and different numbers of monotonic sections are considered. (a) Overhead MV/BPL networks. (b) Overhead LV/BPL networks. (c) Underground MV/BPL networks. (d) Underground LV/BPL networks.

that is responsible for initially estimating the turning points and is adopted in this paper. However, the development of a test similar to [77], which will be tailored to measured BPL coupling functions, would be valuable as future research question.

Although the effectiveness of best L1PMA to coupling transfer function restorations is well presented in the case of suburban, rural, and "LOS" topologies, best L1PMA can have many applications as a data smoothing approach. Despite the large number of local extrema of urban case A and B topologies that can occur during the optimization calculation, the set of an upper bound to the number of monotonic sections may allow a smoother global solution in quadratic complexity with respect to the number of data points [28]. Based on the online available Fortran software package of [33], the indicative processing time in seconds of both the hybrid method and the best L1PMA for Figures 8(a)–8(e), 9(a)–9(e), 10(a)–10(e), and 11(a)–11(e) is reported in Table 2. Despite the high complexity, the computational burden of both the hybrid method and the best L1PMA ranges from 2.230 s to 3.107 s for each distribution BPL topology examined. As the technical characteristics of the system performing the simulations are concerned, it has an Intel Pentium 1.9 GHz CPU and 4 GB RAM. Therefore, the presented data smoothing approach could be a useful intermediate method for real-time processing applications concerning BPL frequency allocation problem [78].

Apart from the visual result of Figures 8(a)–8(j), 9(a)–9(j), 10(a)–10(j), and 11(a)–11(j), the approximation performance of best L1PMA is examined in terms of PES for a number of different fault distributions. More specifically, in Table 3, PES of best L1PMA is compared against fault PES when indicative fault CUDs are applied (i.e., $\alpha_{\mathrm{CUD}} = 3$ dB, $\alpha_{\mathrm{CUD}} = 6$ dB, and $\alpha_{\mathrm{CUD}} = 9$ dB) for the distribution BPL network scenarios of Figures 8(a)–8(j), 9(a)–9(j), 10(a)–10(j), and 11(a)–11(j). Similarly, in Table 4, PES of best L1PMA is compared against fault PES when indicative fault NDs are applied (i.e., $\mu_{\mathrm{ND}} = 0$ dB and $\sigma_{\mathrm{ND}} = 2$ dB, $\mu_{\mathrm{ND}} = 0$ dB and $\sigma_{\mathrm{ND}} = 6$ dB, and $\mu_{\mathrm{ND}} = 0$ dB and $\sigma_{\mathrm{ND}} = 9$ dB) for the same distribution BPL network scenarios.

In Tables 3 and 4, PES, fault PES, and their difference are reported for each distribution BPL network scenario examined. For a given distribution BPL network scenario, when the best L1PMA achieves better PES in comparison with the respective fault PES, the difference is presented in bold; otherwise, it is presented in italic. Apart from small and average faults, best L1PMA is also examined when gross fault cases occur (i.e., CUD with $\alpha_{\mathrm{CUD}} = 9$ dB and ND with $\mu_{\mathrm{ND}} = 0$ dB and $\sigma_{\mathrm{ND}} = 9$ dB). These aggravated cases are denoted by $*$.

Table 2: Indicative processing time of best L1PMA for distribution BPL networks (OV: overhead; UN: underground).

		Urban case A		Urban case B		Suburban case		Rural case		"LOS" case	
		Processing time (s)	Figure	Processing time (s)	Figure	Processing time (s)	Figure	Processing time (s)	Figure	Processing time (s)	Figure
OVMV	WtG[1]	2.230	Figure 8(a)	2.477	Figure 8(b)	2.291	Figure 8(c)	2.407	Figure 8(d)	2.569	Figure 8(e)
OVLV	WtG[1]	2.653	Figure 9(a)	3.107	Figure 9(b)	2.539	Figure 9(c)	2.677	Figure 9(d)	2.677	Figure 9(e)
UNMV	StP[1]	2.644	Figure 10(a)	2.572	Figure 10(b)	2.501	Figure 10(c)	2.624	Figure 10(d)	2.943	Figure 10(e)
UNLV	StP[1]	2.420	Figure 11(a)	2.774	Figure 11(b)	2.592	Figure 11(c)	2.648	Figure 11(d)	2.792	Figure 11(e)

Table 3: PES and PES_{fault} of distribution BPL networks for different fault CUDs (variable α_{CUD}) (OV: overhead; UN: underground).

		α_{CUD}	Urban case A			Urban case B			Suburban case			Rural case			"LOS" case		
			PES (%)	PES_{fault} (%)	Diff. (%)	PES (%)	PES_{fault} (%)	Diff. (%)	PES (%)	PES_{fault} (%)	Diff. (%)	PES (%)	PES_{fault} (%)	Diff. (%)	PES (%)	PES_{fault} (%)	Diff. (%)
OVMV	WtG^1	3 dB	11.3	11.3	**0.0**	8.8	8.8	**0.0**	13.1	13.1	**0.0**	32.6	41.5	**8.9**	36.2	46.0	**9.8**
		6 dB	21.4	22.0	**0.5**	17.1	17.1	**0.0**	35.6	35.6	**0.0**	68.9	93.4	**24.5**	63.8	101.0	**37.2**
		9 dB*	29.1*	30.1*	**1.0***	25.3*	25.3*	**0.0***	54.5*	54.5*	**0.0***	64.7*	105.7*	**41.0***	127.3*	128.2*	**0.9***
	$WtW^{1\text{-}2}$	3 dB	6.7	6.7	**0.0**	6.3	6.3	**0.0**	11.5	11.5	**0.0**	16.5	21.6	**5.1**	12.9	20.1	**7.2**
		6 dB	18.0	18.0	**0.0**	13.6	13.6	**0.0**	22.9	22.9	**0.0**	19.6	35.5	**15.9**	41.5	44.2	**2.7**
		9 dB*	25.7*	25.8*	**0.1***	22.5*	22.5*	**0.0***	28.9*	29.1*	**0.2***	45.4*	54.8*	**9.4***	61.4*	65.8*	**4.4***
OVLV	WtG^1	3 dB	10.7	10.8	**0.1**	8.0	8.0	**0.0**	18.8	18.8	**0.0**	61.6	79.5	**17.9**	41.2	79.9	**38.7**
		6 dB	25.8	28.3	**2.5**	13.4	13.4	**0.0**	41.7	41.7	**0.0**	43.0	103.9	**60.9**	102.6	156.1	**53.5**
		9 dB*	36.1*	36.8*	**0.8***	26.1*	26.1*	**0.0***	73.4*	73.4*	**0.0***	136.9*	195.4*	**58.5***	42.2*	200.0*	**157.8***
	$WtW^{1\text{-}2}$	3 dB	7.9	7.9	**0.0**	7.3	7.3	**0.0**	11.6	11.5	*−0.1*	6.9	25.2	**18.3**	16.6	21.4	**4.8**
		6 dB	15.6	15.6	**0.0**	14.1	14.1	**0.0**	22.6	22.8	**0.2**	11.4	45.8	**34.4**	25.9	36.0	**10.1**
		9 dB*	25.6*	25.8*	**0.2***	23.4*	23.4*	**0.0***	31.3*	31.3*	**0.0***	53.4*	68.2*	**14.8***	43.8*	60.3*	**16.5***
UNMV	StP^1	3 dB	4.9	4.9	**0.0**	4.2	4.2	**0.0**	6.8	6.8	**0.0**	6.7	7.6	**0.9**	7.0	10.1	**3.1**
		6 dB	10.4	10.4	**0.0**	8.3	8.3	**0.0**	13.6	13.6	**0.0**	11.6	16.7	**5.0**	14.2	24.1	**9.9**
		9 dB*	15.4*	15.4*	**0.0***	12.4*	12.4*	**0.0***	18.1*	18.1*	**0.0***	25.7*	25.5*	*−0.2**	15.3*	27.9*	**12.6***
	$PtP^{1\text{-}2}$	3 dB	4.2	4.2	**0.0**	4.2	4.2	**0.0**	5.2	5.2	**0.0**	5.5	6.7	**1.2**	5.2	6.9	**1.7**
		6 dB	7.8	7.8	**0.0**	8.7	8.7	**0.0**	11.0	11.0	**0.0**	10.9	11.7	**0.9**	8.6	12.4	**3.8**
		9 dB*	16.2*	16.2*	**0.0***	10.5*	10.5*	**0.0***	13.7*	13.7*	**0.0***	13.6*	14.9*	**1.3***	9.7*	15.7*	**6.1***
UNLV	StP^1	3 dB	12.2	12.2	**0.0**	6.8	6.8	**0.0**	13.0	13.0	**0.0**	12.9	28.9	**16.1**	24.4	44.3	**19.9**
		6 dB	22.7	22.7	**0.1**	13.3	13.3	**0.0**	33.7	33.7	**0.0**	24.7	59.6	**34.9**	58.9	99.8	**40.9**
		9 dB*	26.1*	26.0*	**0.0***	17.3*	17.3*	**0.0***	44.4*	44.4*	**0.0***	47.5*	87.0*	**39.5***	72.3*	148.1*	**75.8***
	$PtP^{1\text{-}2}$	3 dB	6.9	7.1	**0.2**	6.2	6.2	**0.0**	9.6	9.6	**0.0**	7.6	11.0	**3.4**	10.8	15.3	**4.5**
		6 dB	11.6	12.1	**0.5**	10.1	10.1	**0.0**	18.9	18.9	**0.0**	18.8	24.3	**5.5**	11.9	28.6	**16.7**
		9 dB*	19.5*	20.2*	**0.7***	16.2*	16.2*	**0.0**	28.0*	28.4*	**0.4***	16.3*	38.1*	**21.8***	21.6*	50.0*	**38.7***

Table 4: PES and PES_{fault} of distribution BPL networks for different fault NDs ($\mu_{ND=0}$, variable σ_{ND}) (OV: overhead; UN: underground).

		σ_{ND}	Urban case A			Urban case B			Suburban case			Rural case			"LOS" case		
			PES (%)	PES_{fault} (%)	Diff. (%)	PES (%)	PES_{fault} (%)	Diff. (%)	PES (%)	PES_{fault} (%)	Diff. (%)	PES (%)	PES_{fault} (%)	Diff. (%)	PES (%)	PES_{fault} (%)	Diff. (%)
OVMV	WtG^1	2 dB	11.6	11.6	**0.0**	10.2	10.2	**0.0**	18.5	18.5	**0.0**	36.6	42.0	**5.4**	43.3	48.6	**5.3**
		6 dB	34.9	35.8	**1.0**	23.1	23.1	**0.0**	56.8	56.8	**0.0**	80.3	102.8	**22.5**	100.5	119.2	**18.8**
		9 dB*	49.1*	51.0*	**1.9***	41.4*	41.4*	**0.0***	96.5*	96.5*	**0.0***	214.6*	269.3*	**54.7***	147.2*	179.9*	**32.7***
	$WtW^{1\text{-}2}$	2 dB	9.0	9.2	**0.2**	7.4	7.4	**0.0**	18.0	18.0	**0.0**	20.9	28.7	**7.8**	13.3	21.1	**7.9**
		6 dB	26.1	27.3	**1.1**	25.0	25.0	**0.0**	43.2	43.2	**0.0**	49.1	62.9	**13.8**	60.5	67.1	**6.6**
		9 dB*	37.7*	36.6*	*−1.1**	32.6*	32.6*	**0.0***	61.2*	61.2*	**0.0***	63.7*	77.8*	**14.1***	94.2*	102.8*	**8.6***
OVLV	WtG^1	2 dB	12.4	12.9	**0.5**	8.0	8.0	**0.0**	17.2	17.2	**0.0**	28.7	61.6	**32.8**	41.4	84.4	**43.1**
		6 dB	34.2	36.7	**2.5**	27.5	27.5	**0.0**	48.8	48.8	**0.0**	75.6	181.5	**105.9**	111.2	254.3	**143.1**
		9 dB*	54.6*	58.1*	**3.5***	36.5*	36.5*	**0.0***	79.9*	79.9*	**0.0***	232.3*	393.9*	**161.6***	147.1*	353.9*	**206.8***
	$WtW^{1\text{-}2}$	2 dB	8.1	8.5	**0.3**	6.8	6.8	**0.0**	12.6	12.6	**0.0**	5.2	20.1	**14.8**	15.4	26.5	**11.1**
		6 dB	31.7	30.8	*−0.9*	19.1	19.1	**0.0**	36.4	26.8	**0.4**	14.9	75.9	**61.0**	27.3	67.3	**40.0**
		9 dB*	40.0*	40.0*	**0.0***	27.4*	27.4*	**0.0***	53.4*	53.4*	**0.0***	48.1*	98.0*	**50.0***	62.9*	118.4*	**55.5***
UNMV	StP^1	2 dB	4.0	4.0	**0.0**	5.8	5.9	**0.1**	6.7	6.7	**0.0**	8.9	10.7	**1.9**	5.5	8.8	**3.3**
		6 dB	21.3	21.3	**0.0**	10.7	10.5	*−0.2*	23.0	23.0	**0.0**	17.4	22.5	**5.1**	12.2	25.1	**12.9**
		9 dB*	23.8*	23.8*	**0.0***	23.2*	23.2*	**0.0***	35.4*	35.4*	**0.0***	24.2*	34.4*	**10.2***	25.1*	38.1*	**12.9***
	$PtP^{1\text{-}2}$	2 dB	4.1	4.1	**0.0**	3.9	3.9	**0.0**	5.6	5.6	**0.0**	7.2	7.2	**0.0**	4.6	7.1	**2.4**
		6 dB	18.4	18.4	**0.0**	13.1	12.9	*−0.2*	13.2	13.2	**0.0**	15.3	16.0	**0.8**	14.9	20.1	**5.2**
		9 dB*	21.3*	21.3*	**0.0***	19.5*	19.5*	**0.0***	20.5*	20.5*	**0.0***	30.3*	34.3*	**4.0***	13.1*	29.0*	**15.9***
UNLV	StP^1	2 dB	10.2	10.6	**0.3**	9.0	9.0	**0.0**	18.0	18.0	**0.0**	15.7	29.0	**13.3**	23.3	59.6	**36.6**
		6 dB	30.2	30.6	**0.4**	20.4	20.4	**0.0**	44.0	44.0	**0.0**	29.0	74.8	**45.8**	25.5	105.1	**79.6**
		9 dB*	58.8*	62.2*	**3.3***	31.1*	31.6*	**0.6***	69.4*	66.4*	*−3.0**	66.9*	150.1*	**83.2***	58.7*	224.0*	**165.3***
	$PtP^{1\text{-}2}$	2 dB	8.4	8.4	**0.0**	5.6	5.6	**0.0**	9.0	9.0	**0.0**	7.6	13.4	**5.8**	7.9	14.6	**6.7**
		6 dB	20.5	20.6	**0.1**	15.8	15.8	**0.0**	29.1	29.1	**0.0**	16.4	42.3	**25.9**	19.1	35.5	**16.4**
		9 dB*	34.4*	34.4*	**0.0***	23.6*	23.6*	**0.0***	46.2*	46.5*	**0.3***	32.2*	71.2*	**39.0***	25.5*	70.2*	**92.9***

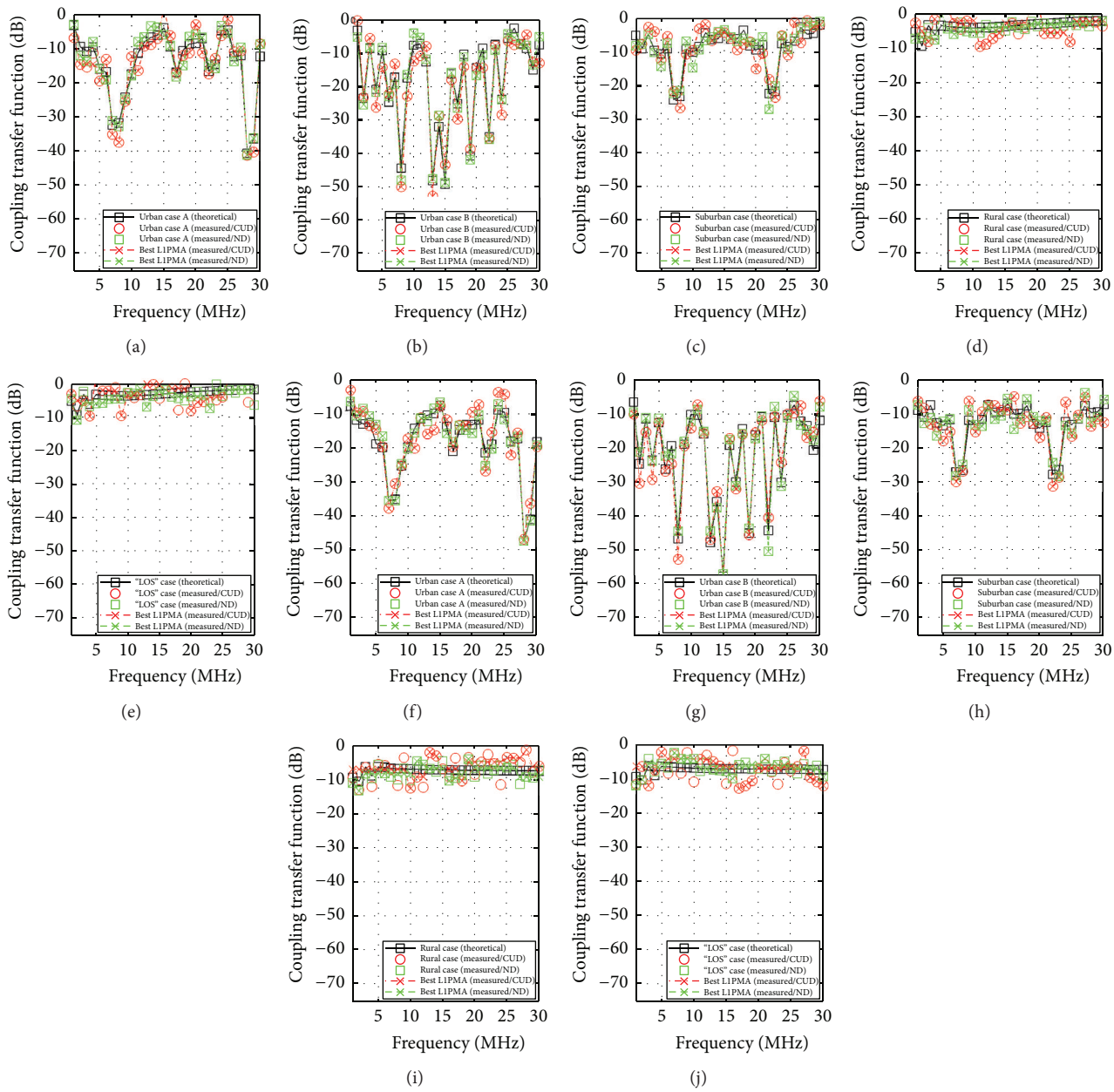

Figure 8: Theoretical, measured, and best L1PMA coupling transfer function of the five indicative topologies of overhead MV/BPL networks for two indicative fault distributions (CUD and NU) when different coupling schemes are applied. (a)–(e) WtG^1 coupling scheme. (f)–(j) $WtW^{1\text{-}2}$ coupling scheme.

From Tables 3 and 4, it is obvious that best L1PMA achieves remarkably mitigating the faults that occurred which follow either CUD or ND. More specifically, in 96.7% and 93.3% of the examined distribution BPL network scenarios that suffer from faults following CUD and ND, respectively, best L1PMA has achieved average PES improvement equal to 9% and 15.8%, respectively.

Further analyzing the data of Tables 3 and 4, in the rural and "LOS" cases where best L1PMA achieves its best results, the average PES improvement is equal to 25.4% and 36%, respectively. More analytically, in the rural cases, best L1PMA achieves average PES improvement of 18.3% and 32.5% when faults follow CUD and ND, respectively. The same results are presented in "LOS" cases where best L1PMA achieves average PES improvement of 26.1% and 46% when faults follow CUD and ND, respectively. These significant PES improvements are explained by the fact that the coupling transfer functions of rural and "LOS" cases maintain relatively steady inclination due to the "LOS" attenuation with shallow or no spectral notches, respectively. On the basis of the low optimal number of monotonic sections for these cases, best L1PMA focuses on the most important local extrema and the general form of the curve neglecting the fluctuations due to several faults.

Now, as concerns the behavior of best L1PMA against gross errors, best L1PMA is characterized by its remarkable property to ignore the presence as well as the magnitude

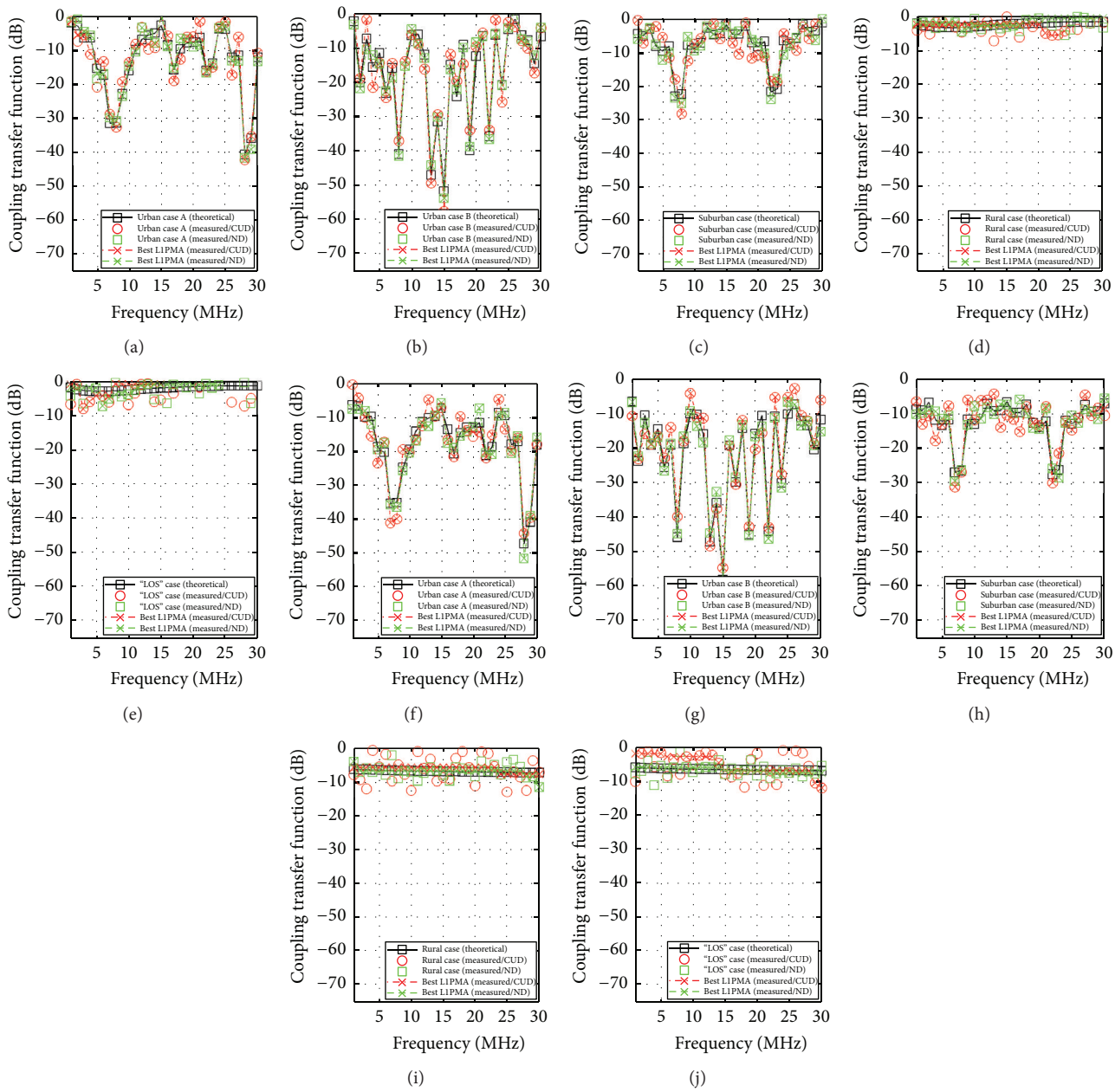

FIGURE 9: Same as in Figures 8(a)–8(j) but for overhead LV/BPL networks.

of these gross errors during the determination of the best fit in all the cases examined. More specifically, best L1PMA achieves average PES improvement equal to 13.8% and 26.4% when the gross faults that occurred follow CUD (i.e., $\alpha_{\mathrm{CUD}} = 9$ dB) and ND (i.e., $\mu_{\mathrm{ND}} = 0$ dB and $\sigma_{\mathrm{ND}} = 9$ dB), respectively. Compared to the overall average PES improvement that is equal to 9% and 15.8%, when the faults that occurred follow CUD and ND, respectively, best L1PMA is specialized with the mitigation of the gross faults.

Synoptically, it is evident that the fault magnitude affects the approximation efficacy of best L1PMA to the coupling transfer functions of distribution BPL networks. In order to highlight this factor influence, PES is plotted versus the maximum value α_{CUD} of CUD in Figure 12(a) for the five indicative topologies of overhead MV/BPL networks when WtG^1 and $\mathrm{WtW}^{1\text{-}2}$ coupling schemes are considered. In Figures 12(b)–12(d), the same plots are given in the case of overhead LV/BPL, underground MV/BPL, and underground LV/BPL networks, respectively. Note that, in the case of underground distribution BPL networks, StP^1 or $\mathrm{PtP}^{1\text{-}2}$ coupling schemes are applied instead of WtG^1 or $\mathrm{WtW}^{1\text{-}2}$ ones, respectively.

Similar to Figures 12(a)–12(d), PES is plotted versus the standard deviation σ_{ND} in Figure 13(a) for overhead MV/BPL, overhead LV/BPL, underground MV/BPL, and underground LV/BPL networks, respectively. Note that in all the cases examined the mean μ_{ND} remains equal to 0 (unbiased ND).

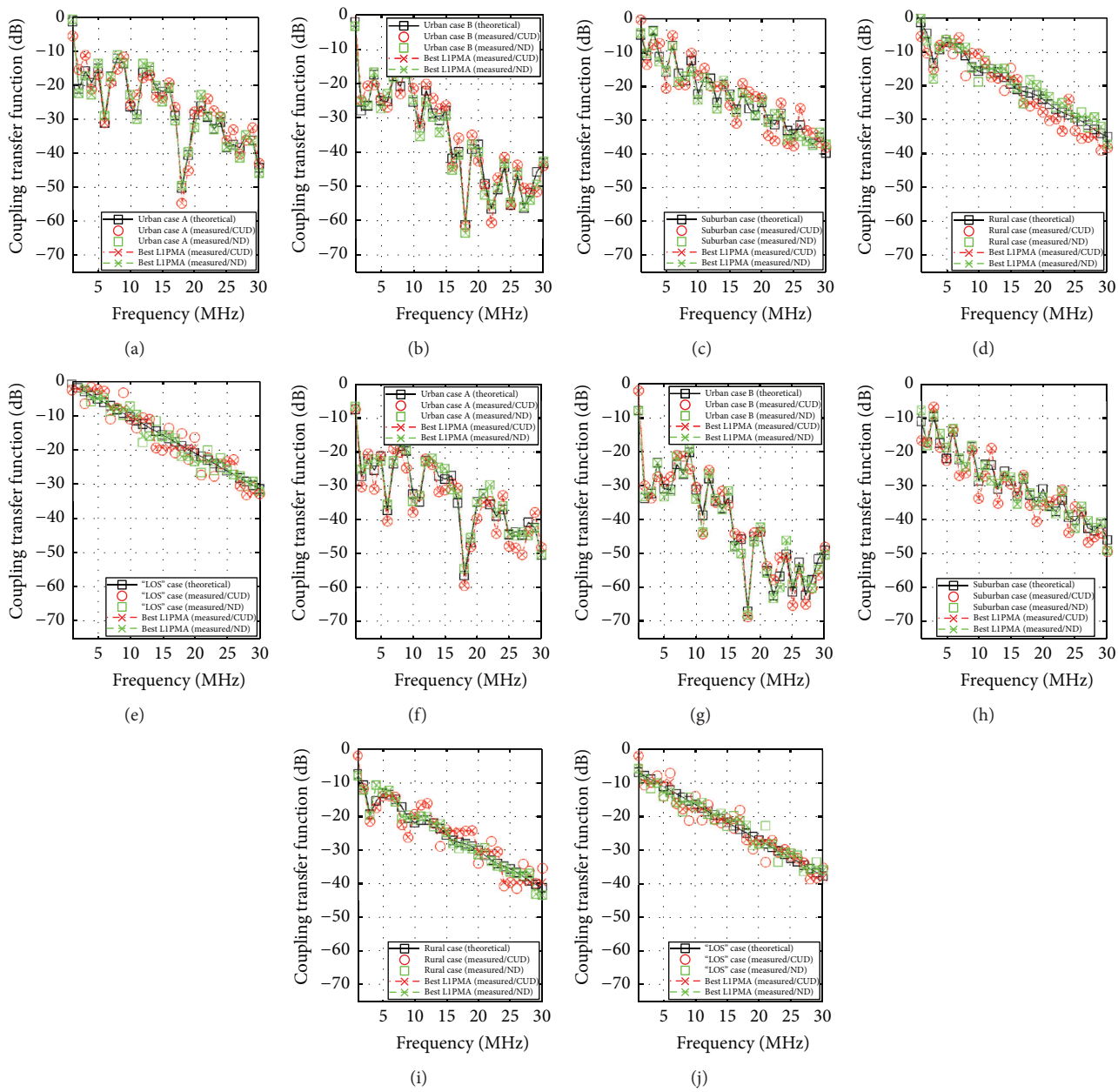

Figure 10: Theoretical, measured, and best L1PMA coupling transfer function of the five indicative topologies of underground MV/BPL networks for two indicative fault distributions (CUD and NU) when different coupling schemes are applied. (a)–(e) StP^1 coupling scheme. (f)–(j) $PtP^{1\text{-}2}$ coupling scheme.

From Figures 13(a)–13(d), it is obvious that PES primarily depends on the CUD maximum value and ND standard deviation. Also, for the same value of CUD maximum value and ND standard deviation, PES is more sensitive to the fluctuations of ND standard deviation.

Independently of the fault distribution, PES of overhead distribution BPL networks is more fault vulnerable in comparison with PES of underground distribution BPL networks. This is due to the fact that overhead BPL networks suffer from reflections due to the multipath environment rather than the "LOS" attenuation. Since their average channel attenuation is significantly lower than the respective one of underground BPL networks, the same fault magnitude more crucially harms the coupling transfer functions of overhead BPL networks further deteriorating their PES. Nevertheless, as concerns PES differences between MV and LV BPL networks of the same grid type (either overhead or underground), these differences remain marginal.

Except for the distribution power grid type, significant PES differences are shown among the different topologies. More specifically, in overhead distribution BPL networks, rural and "LOS" topologies are the most fault sensitive whereas, in underground distribution BPL networks, urban case A and B topologies are the most fault resistant. This is due

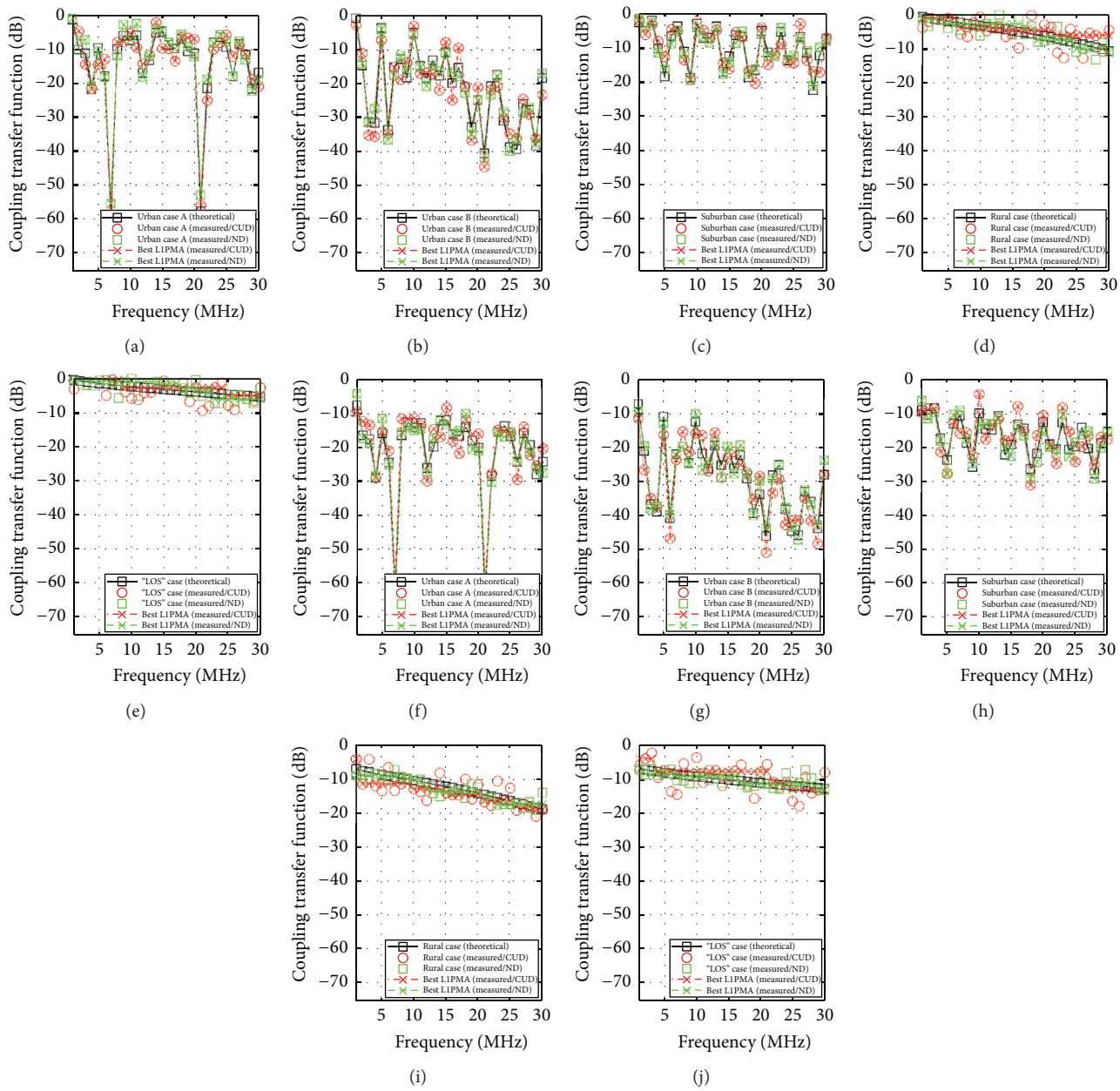

Figure 11: Same as in Figures 10(a)–10(j) but for underground LV/BPL networks.

to the fact that even if coupling transfer functions of rural and "LOS" topologies maintain relatively stable inclination due to their "LOS" attenuation, a plethora of faults can abrupt the best fit of best L1PMA by adding a fixed difference between theoretical and approximated coupling transfer functions across the examined frequency band. Consequently, the high optimal number of monotonic sections locally isolates the effect of the faults that occurred resulting in a biased best fit result.

Moreover, comparing the PES performance among different coupling schemes, WtW and PtP coupling schemes present lower PES than the respective WtG and StP ones. This is due to the fact that WtW and PtP coupling transfer functions present lower attenuation values in comparison with the respective WtG and StP ones further affecting their PES performance.

Concluding the analysis of Section 4, the primary advantage of best L1PMA against least square monotonicity algorithms has been clearly highlighted; in accordance with [60], best L1PMA smooths the data without (i) creating ringing and blurring artifacts around transfer function plots and (ii) inducing round-off error in the modified data [29, 59, 60, 76]. This is due to the fact that, during the calculation of the best L1PMA, the arithmetic operations involved are mainly comparisons so that the median of data of each monotonic section is estimated.

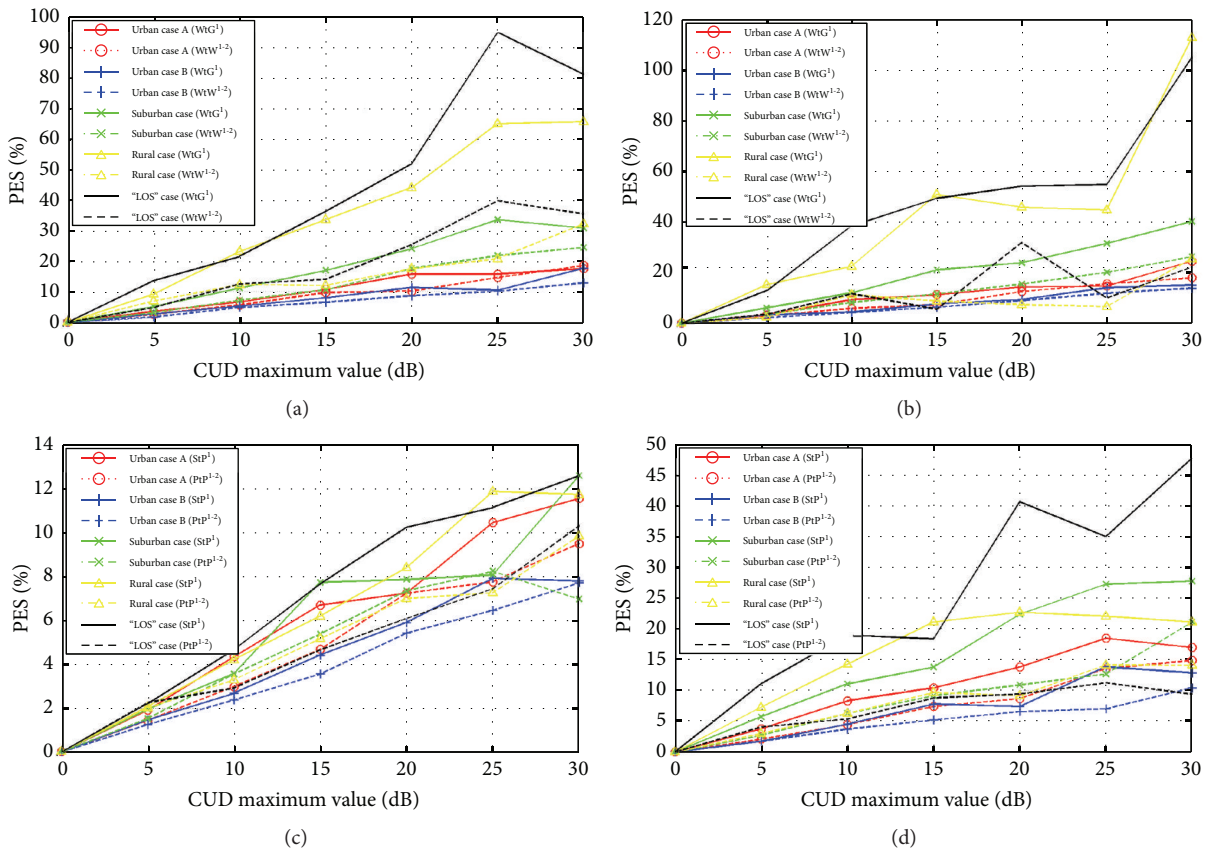

Figure 12: PES of distribution BPL topologies when various coupling schemes are applied and different fault CUDs (variable maximum value α_{CUD}) are considered. (a) Overhead MV/BPL networks. (b) Overhead LV/BPL networks. (c) Underground MV/BPL networks. (d) Underground LV/BPL networks.

5. Conclusions

Among the wide range of applications that best L1PMA is relevant to, an application of best L1PMA to approximate and to mitigate faults during the determination of transfer functions of distribution BPL networks has been proposed in this paper. To assess the performance of best L1PMA, PES metric has been used allowing (i) the evaluation of the approximation accuracy of the best L1PMA to the theoretical coupling transfer functions and (ii) the evaluation of the restoration of the theoretical coupling transfer functions when faults occur.

Despite the large number and the extent of the notches (local extrema) due to the multipath environment, the steady inclination due to the "LOS" attenuation, and the burst mode of the assumed faults during the measurements, best L1PMA has successfully mitigated all the previous deficiencies in all the examined distribution BPL networks. More analytically, in the case of transfer functions of distribution BPL networks with no faults, best L1PMA has achieved average PES equal to 0.99×10^{-5}%. In the case of transfer functions of distribution BPL networks with faults that follow CUD and ND, best L1PMA has achieved average PES improvement equal to 12.4%. Note that the average PES improvement can surpass 25.4% when gross faults occur.

Taking into consideration the diverse nature of distribution BPL topologies and the performance of best L1PMA as a fault counteracting technique, best L1PMA can operate as the necessary intermediate antifault method between the measurement phase and the theoretical data processing.

Nomenclature

MV:	Medium-voltage
LV:	Low-voltage
SG:	Smart grid
BPL:	Broadband over power lines
IP:	Internet protocol
MTL:	Multiconductor transmission line
Best L1PMA:	Best L1 piecewise monotonic data approximation
PES:	Percent error sum
ACSR:	Aluminium conductor steel reinforced
PILC:	Paper-insulated lead cable
XLPE:	Cross-linked polyethylene
LOS:	Line of Sight
TL:	Transmission line
CUD:	Continuous uniform distribution
ND:	Normal distribution.

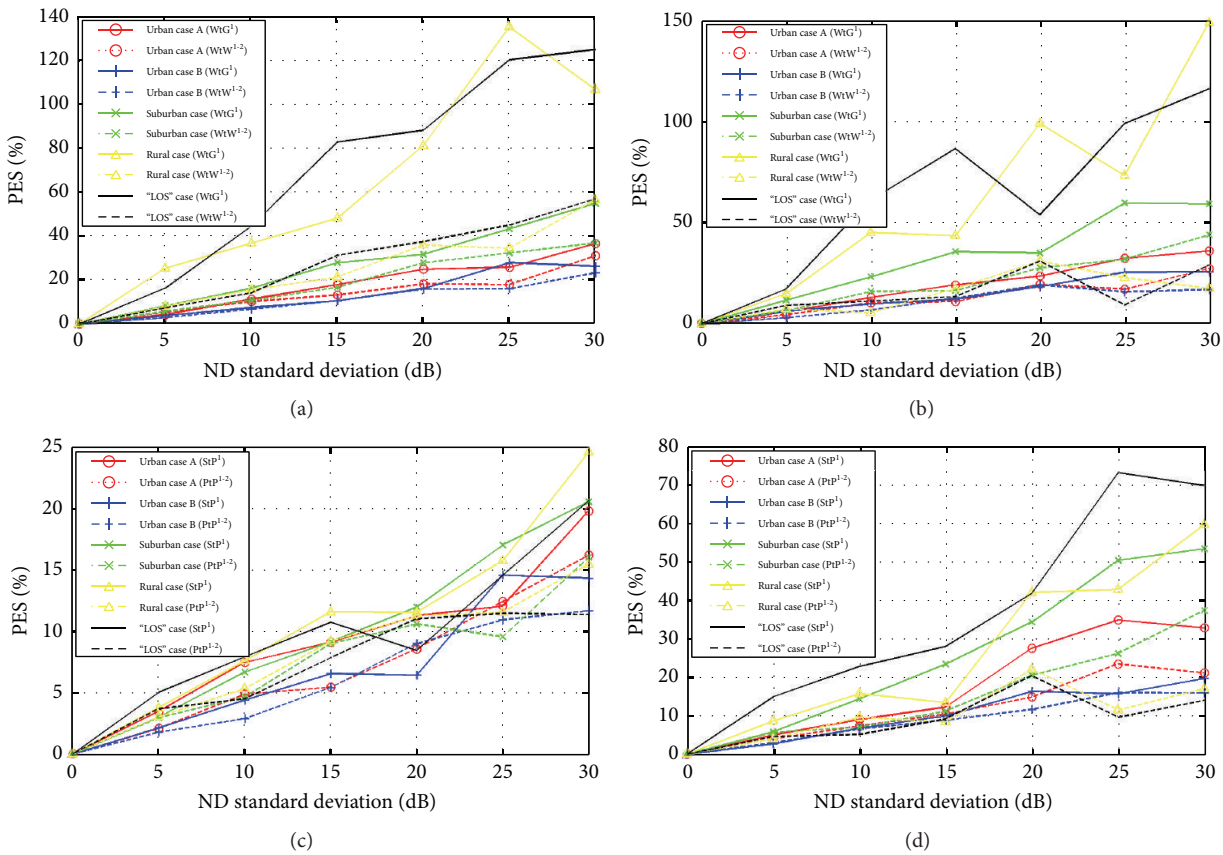

FIGURE 13: PES of distribution BPL topologies when various coupling schemes are applied and different fault NDs (mean $\mu_{ND} = 0$ and variable standard deviation σ_{ND}) are considered. (a) Overhead MV/BPL networks. (b) Overhead LV/BPL networks. (c) Underground MV/BPL networks. (d) Underground LV/BPL networks.

Competing Interests

The author declares that there are no competing interests.

References

[1] A. G. Lazaropoulos, "Review and progress towards the capacity boost of overhead and underground medium-voltage and low-voltage broadband over power lines networks: cooperative communications through two- and three-hop repeater systems," *ISRN Electronics*, vol. 2013, Article ID 472190, 19 pages, 2013.

[2] G. T. Heydt, C. C. Liu, A. G. Phadke, and V. Vittal, "Solutions for the crisis in electric power supply," *IEEE Computer Applications in Power*, vol. 14, no. 3, pp. 22–30, 2001.

[3] H. Farhangi, "The path of the smart grid," *IEEE Power and Energy Magazine*, vol. 8, no. 1, pp. 18–28, 2010.

[4] A. G. Lazaropoulos, "Towards modal integration of overhead and underground low-voltage and medium-voltage power line communication channels in the smart grid landscape: model expansion, broadband signal transmission characteristics, and statistical performance metrics (invited paper)," *ISRN Signal Processing*, vol. 2012, Article ID 121628, 17 pages, 2012.

[5] R. Schneiderman, "Smart grid represents a potentially huge market for the electronics industry [special reports]," *IEEE Signal Processing Magazine*, vol. 27, no. 5, pp. 8–15, 2010.

[6] S. Galli, A. Scaglione, and Z. Wang, "For the grid and through the grid: the role of power line communications in the smart grid," *Proceedings of the IEEE*, vol. 99, no. 6, pp. 998–1027, 2011.

[7] A. G. Lazaropoulos and P. Lazaropoulos, "Financially stimulating local economies by exploiting communities' microgrids: power trading and Hybrid Techno-Economic (HTE) model," *Trends in Renewable Energy*, vol. 1, no. 3, pp. 131–184, 2015.

[8] A. Haidine, B. Adebisi, A. Treytl, H. Pille, B. Honary, and A. Portnoy, "High-speed narrowband PLC in smart grid landscape—state-of-the-art," in *Proceedings of the IEEE International Symposium on Power Line Communications and Its Applications (ISPLC '11)*, pp. 468–473, Udine, Italy, April 2011.

[9] A. G. Lazaropoulos, "Numerical evaluation of broadband transmission characteristics of underground low-voltage networks—introducing techno-pedagogical (TP) method," *International Journal of Electrical Power and Energy Systems*, vol. 55, pp. 253–260, 2014.

[10] A. G. Lazaropoulos, "Wireless sensor network design for transmission line monitoring, metering, and controlling: introducing Broadband over Power Lines-Enhanced Network Model (BPLeNM)," *ISRN Power Engineering*, vol. 2014, Article ID 894628, 22 pages, 2014.

[11] A. G. Lazaropoulos, "Wireless sensors and broadband over powerlines networks: the performance of broadband over powerlines-enhanced network model (BPLeNM) (invited paper)," *ICAS Publishing Group Transaction on IoT and Cloud*

Computing, vol. 2, no. 3, pp. 1–35, 2014, http://icas-pub.org/ojs/index.php/ticc/article/view/27/17.

[12] A. G. Lazaropoulos, "Policies for carbon energy footprint reduction of overhead multiple-input multiple-output high voltage broadband over power lines networks," *Trends in Renewable Energy*, vol. 1, no. 2, pp. 87–118, 2015.

[13] A. G. Lazaropoulos and P. G. Cottis, "Transmission characteristics of overhead medium-voltage power-line communication channels," *IEEE Transactions on Power Delivery*, vol. 24, no. 3, pp. 1164–1173, 2009.

[14] A. G. Lazaropoulos and P. G. Cottis, "Capacity of overhead medium voltage power line communication channels," *IEEE Transactions on Power Delivery*, vol. 25, no. 2, pp. 723–733, 2010.

[15] A. G. Lazaropoulos and P. G. Cottis, "Broadband transmission via underground medium-voltage power lines—part I: transmission characteristics," *IEEE Transactions on Power Delivery*, vol. 25, no. 4, pp. 2414–2424, 2010.

[16] A. G. Lazaropoulos and P. G. Cottis, "Broadband transmission via underground medium-voltage power lines—part II: capacity," *IEEE Transactions on Power Delivery*, vol. 25, no. 4, pp. 2425–2434, 2010.

[17] A. G. Lazaropoulos, "Factors influencing broadband transmission characteristics of underground low-voltage distribution networks," *IET Communications*, vol. 6, no. 17, pp. 2886–2893, 2012.

[18] A. G. Lazaropoulos, "Review and progress towards the common broadband management of high-voltage transmission grids: model expansion and comparative modal analysis," *ISRN Electronics*, vol. 2012, Article ID 935286, 18 pages, 2012.

[19] A. G. Lazaropoulos, "Towards broadband over power lines systems integration: transmission characteristics of underground low-voltage distribution power lines," *Progress in Electromagnetics Research B*, no. 39, pp. 89–114, 2012.

[20] A. G. Lazaropoulos, "Broadband transmission characteristics of overhead high-voltage power line communication channels," *Progress in Electromagnetics Research B*, vol. 36, pp. 373–398, 2012.

[21] A. G. Lazaropoulos, "Broadband transmission and statistical performance properties of overhead high-voltage transmission networks," *Journal of Computer Networks and Communications*, vol. 2012, Article ID 875632, 16 pages, 2012.

[22] T. A. Papadopoulos, A. I. Chrysochos, and G. K. Papagiannis, "Narrowband power line communication: medium voltage cable modeling and laboratory experimental results," *Electric Power Systems Research*, vol. 102, pp. 50–60, 2013.

[23] A. N. Milioudis, G. T. Andreou, and D. P. Labridis, "Enhanced protection scheme for smart grids using power line communications techniques—part II: location of high impedance fault position," *IEEE Transactions on Smart Grid*, vol. 3, no. 4, pp. 1631–1640, 2012.

[24] T. A. Papadopoulos, C. G. Kaloudas, A. I. Chrysochos, and G. K. Papagiannis, "Application of narrowband power-line communication in medium-voltage smart distribution grids," *IEEE Transactions on Power Delivery*, vol. 28, no. 2, pp. 981–988, 2013.

[25] Y.-H. Kim, S. Choi, S.-C. Kim, and J.-H. Lee, "Capacity of OFDM two-hop relaying systems for medium-voltage powerline access networks," *IEEE Transactions on Power Delivery*, vol. 27, no. 2, pp. 886–894, 2012.

[26] J.-H. Lee and Y.-H. Kim, "Diversity relaying for parallel use of power-line and wireless communication networks," *IEEE Transactions on Power Delivery*, vol. 29, no. 3, pp. 1301–1310, 2014.

[27] I. C. Demetriou and M. J. D. Powell, "Least squares smoothing of univariate data to achieve piecewise monotonicity," *IMA Journal of Numerical Analysis*, vol. 11, no. 3, pp. 411–432, 1991.

[28] I. C. Demetriou and V. Koutoulidis, "On signal restoration by piecewise monotonic data approximation," in *Proceedings of the World Congress on Engineering (WCE '13)*, pp. 268–273, London, UK, July 2013.

[29] I. C. Demetriou, "An application of best L_1 piecewise monotonic data approximation to signal restoration," *IAENG International Journal of Applied Mathematics*, vol. 53, no. 4, pp. 226–232, 2013.

[30] I. C. Demetriou, "L1PMA: a Fortran 77 package for best L_1 piecewise monotonic data smoothing," *Computer Physics Communications*, vol. 151, no. 3, pp. 315–338, 2003.

[31] I. C. Demetriou, *Data smoothing by piecewise monotonic divided differences [Ph.D. thesis]*, Department of Applied Mathematics and Theoretical Physics, University of Cambridge, Cambridge, UK, 1985.

[32] I. C. Demetriou, "Best L1 piecewise monotonic data modelling," *International Transactions in Operational Research*, vol. 1, no. 1, pp. 85–94, 1994.

[33] http://cpc.cs.qub.ac.uk/summaries/ADRF.

[34] P. Amirshahi and M. Kavehrad, "High-frequency characteristics of overhead multiconductor power lines for broadband communications," *IEEE Journal on Selected Areas in Communications*, vol. 24, no. 7, pp. 1292–1303, 2006.

[35] P. Amirshahi, *Broadband access and home networking through powerline networks [Ph.D. thesis]*, The Pennsylvania-State University, State College, Pa, USA, 2006.

[36] M. D'Amore and M. S. Sarto, "A new formulation of lossy ground return parameters for transient analysis of multiconductor dissipative lines," *IEEE Transactions on Power Delivery*, vol. 12, no. 1, pp. 303–314, 1997.

[37] P. C. J. M. van der Wielen, *On-line detection and location of partial discharges in medium-voltage power cables [Ph.D. dissertation]*, Eindhoven University of Technology, Eindhoven, The Netherlands, 2005, http://alexandria.tue.nl/extra2/200511097.pdf.

[38] OPERA1, "D44: report presenting the architecture of plc system, the electricity network topologies, the operating modes and the equipment over which PLC access system will be installed," IST Integrated Project 507667, 2005.

[39] T. Sartenaer, *Multiuser communications over frequency selective wired channels and applications to the powerline access network [Ph.D. thesis]*, Université Catholique de Louvain, Louvain-la-Neuve, Belgium, 2004.

[40] T. Sartenaer and P. Delogne, "Powerline cables modelling for broadband communications," in *Proceedings of the IEEE International Conference on Power Line Communications and its Applications (ISPLC '01)*, pp. 331–337, Malmö, Sweden, April 2001.

[41] T. Mengcong and Z. Mingyue, "Research of transmission parameters of four-conductor cables for power line communication," in *Proceedings of the International Conference on Computer Science and Software Engineering (CSSE '08)*, vol. 5, pp. 1306–1309, Wuhan, China, December 2008.

[42] N. Theethayi, *Electromagnetic interference in distributed outdoor electrical systems, with an emphasis on lightning interaction with electrified railway network [Ph.D. dissertation]*, Uppsala University, Uppsala, Sweden, 2005.

[43] J. Anatory, N. Theethayi, R. Thottappillil, M. M. Kissaka, and N. H. Mvungi, "The influence of load impedance, line length, and branches on underground cable Power-Line Communications (PLC) systems," *IEEE Transactions on Power Delivery*, vol. 23, no. 1, pp. 180–187, 2008.

[44] J. Anatory, N. Theethayi, and R. Thottappillil, "Power-line communication channel model for interconnected networks—part II: multiconductor system," *IEEE Transactions on Power Delivery*, vol. 24, no. 1, pp. 124–128, 2009.

[45] J. Anatory, N. Theethayi, R. Thottappillil, M. M. Kissaka, and N. H. Mvungi, "The effects of load impedance, line length, and branches in typical low-voltage channels of the BPLC systems of developing countries: transmission-line analyses," *IEEE Transactions on Power Delivery*, vol. 24, no. 2, pp. 621–629, 2009.

[46] A. G. Lazaropoulos, "Deployment concepts for overhead high voltage broadband over power lines connections with two-hop repeater system: capacity countermeasures against aggravated topologies and high noise environments," *Progress in Electromagnetics Research B*, vol. 44, pp. 283–307, 2012.

[47] T. Calliacoudas and F. Issa, "Multiconductor transmission lines and cables solver, an efficient simulation tool for PL channel networks development," in *Proceedings of the IEEE International Conference on Power Line Communications and Its Applications (ISPLC '02)*, Athens, Greece, March 2002.

[48] S. Galli and T. Banwell, "A novel approach to the modeling of the indoor power line channel—part II: transfer function and its properties," *IEEE Transactions on Power Delivery*, vol. 20, no. 3, pp. 1869–1878, 2005.

[49] H. Meng, S. Chen, Y. L. Guan et al., "Modeling of transfer characteristics for the broadband power line communication channel," *IEEE Transactions on Power Delivery*, vol. 19, no. 3, pp. 1057–1064, 2004.

[50] X. Cheng, R. Cao, and L. Yang, "On the system capacity of relay-aided Powerline Communications," in *Proceedings of the IEEE International Symposium on Power Line Communications and Its Applications (ISPLC '11)*, pp. 170–175, Udine, Italy, April 2011.

[51] V. B. Balakirsky and A. J. Han Vinck, "Potential performance of PLC systems composed of several communication links," in *Proceedings of the 9th International Symposium on Power Line Communications and Its Applications (ISPLC '05)*, pp. 12–16, IEEE, Vancouver, Canada, April 2005.

[52] S. Galli and T. C. Banwell, "A deterministic frequency-domain model for the indoor power line transfer function," *IEEE Journal on Selected Areas in Communications*, vol. 24, no. 7, pp. 1304–1316, 2006.

[53] A. Cataliotti, A. Daidone, and G. Tinè, "Power line communication in medium voltage systems: characterization of MV cables," *IEEE Transactions on Power Delivery*, vol. 23, no. 4, pp. 1896–1902, 2008.

[54] A. M. Tonello, F. Versolatto, B. Béjar, and S. Zazo, "A fitting algorithm for random modeling the PLC channel," *IEEE Transactions on Power Delivery*, vol. 27, no. 3, pp. 1477–1484, 2012.

[55] J. Anatory, N. Theethayi, R. Thottappillil, M. M. Kissaka, and N. H. Mvungi, "The effects of load impedance, line length, and branches in the BPLC—transmission-line analysis for indoor voltage channel," *IEEE Transactions on Power Delivery*, vol. 22, no. 4, pp. 2150–2155, 2007.

[56] M. Kuhn, S. Berger, I. Hammerström, and A. Wittneben, "Power line enhanced cooperative wireless communications," *IEEE Journal on Selected Areas in Communications*, vol. 24, no. 7, pp. 1401–1410, 2006.

[57] T. Banwell and S. Galli, "A novel approach to the modeling of the indoor power line channel part I: circuit analysis and companion model," *IEEE Transactions on Power Delivery*, vol. 20, no. 2, pp. 655–663, 2005.

[58] A. P. Bruner, K. Scott, D. Wilson et al., *Automatic Peak Finding of Dynamic Batch Sets of Low SNR In-Vivo Phosphorus NMR Spectra*, Departments of Radiology, Physics, Nuclear and Radiological Sciences, Surgery, Mathematics, Medicine, and Exercise and Sport Sciences, University of Florida, and the Veterans Affairs Medical Center, Gainesville, Fla, USA, 1998, http://cds.ismrm.org/ismrm-1998/PDF7/P1857.PDF.

[59] J. Lu, "Signal restoration with controlled piecewise monotonicity constraint," in *Proceedings of the IEEE International Conference on Acoustics, Speech and Signal Processing (ICASSP '98)*, vol. 3, pp. 1621–1624, Seattle, Wash, USA, May 1998.

[60] J. B. Weaver, "Applications of monotonic noise reduction algorithms in fMRI, phase estimation, and contrast enhancement," *International Journal of Imaging Systems and Technology*, vol. 10, no. 2, pp. 177–185, 1999.

[61] J. G. Proakis and D. G. Manolakis, *Digital Signal Processing: Principles, Algorithms and Applications*, Prentice Hall, Upper Saddle River, NJ, USA, 4th edition, 2006.

[62] R. C. Gonzalez and R. E. Woods, *Digital Image Processing*, Pearson Prentice Hall, Upper Saddle River, NJ, USA, 3rd edition, 2008.

[63] A. G. Lazaropoulos, *Engineering the Art through the Lens of L1PMA: A Tribute to the Modern Greek Painters*, Art Book ISSUU Digital Publishing Platform, 2014, http://issuu.com/lazaropoulos/docs/l1pma.

[64] A. G. Lazaropoulos, "ReEngineering the Art through the Lens of L2WPMA: A Tribute to Leonardo da Vinci's Inventions: Flying Machines, War Machines, Architect/Innovations and Water Land Machines," Art Book ISSUU Digital Publishing Platform, November 2014, https://issuu.com/lazaropoulos/docs/l2wpma/1.

[65] A. G. Lazaropoulos, *ReEngineering the Art through the Lens of L1PMA & L2WPMA: The Eternal Youth of the Parthenon Art, Architecture, Marble Sculpture, Metallurgy Pottery*, Art Book ISSUU Digital Publishing Platform, 2014, http://issuu.com/lazaropoulos/docs/l1pma_l2wpma.

[66] J. Shin and J. Jeong, "Improved outage probability of indoor PLC system for multiple users using resource allocation algorithms," *IEEE Transactions on Power Delivery*, vol. 28, no. 4, pp. 2228–2235, 2013.

[67] M. Ur Rehman, S. Wang, Y. Liu, S. Chen, X. Chen, and C. G. Parini, "Achieving high data rate in multiband-OFDM UWB over power-line communication system," *IEEE Transactions on Power Delivery*, vol. 27, no. 3, pp. 1172–1177, 2012.

[68] A. Cataliotti, D. Di Cara, R. Fiorelli, and G. Tinè, "Power-line communication in medium-voltage system: simulation model and onfield experimental tests," *IEEE Transactions on Power Delivery*, vol. 27, no. 1, pp. 62–69, 2012.

[69] K.-H. Kim, H.-B. Lee, Y.-H. Kim, J.-H. Lee, and S.-C. Kim, "Cooperative multihop AF relay protocol for medium-voltage power-line-access network," *IEEE Transactions on Power Delivery*, vol. 27, no. 1, pp. 195–204, 2012.

[70] P. Pagani, A. Ismail, and A. Zeddam, "Path identification in a power-line network based on channel transfer function measurements," *IEEE Transactions on Power Delivery*, vol. 27, no. 3, pp. 1081–1089, 2012.

[71] A. G. Lazaropoulos, "Broadband over power lines systems convergence: multiple-input multiple-output communications

analysis of overhead and underground low-voltage and medium-voltage BPL networks," *ISRN Power Engineering*, vol. 2013, Article ID 517940, 30 pages, 2013.

[72] C. de Boor, *A Practical Guide to Splines*, vol. 27 of *Applied Mathematical Sciences*, Springer, New York, NY, USA, 2001.

[73] M. Holschneider, *Wavelets. An Analysis Tool*, Clarendon Press, Oxford, UK, 1997.

[74] M. J. D. Powell, *Approximation Theory and Methods*, Cambridge University Press, Cambridge, UK, 1981.

[75] A. G. Lazaropoulos, "Overhead and underground MIMO low voltage broadband over power lines networks and EMI regulations: towards greener capacity performances," *Computers and Electrical Engineering*, vol. 39, no. 7, pp. 2214–2230, 2013.

[76] J. Lu, "Consistent signal reconstruction from wavelet extrema representation," in *Wavelet Applications in Signal and Image Processing V*, vol. 3169 of *Proceedings of SPIE*, October 1997.

[77] E. Vassiliou and I. C. Demetriou, "An adaptive algorithm for least squares piecewise monotonic data fitting," *Computational Statistics & Data Analysis*, vol. 49, no. 2, pp. 591–609, 2005.

[78] I. C. Demetriou, "Discrete piecewise monotonic approximation by a strictly convex distance function," *Mathematics of Computation*, vol. 64, no. 209, pp. 157–180, 1995.